

PREPARATION AND OPERATIONS OF THE MISSION PERFORMANCE  
CENTRE (MPC) FOR THE COPERNICUS SENTINEL-3 MISSION

**S3-A OLCI Cyclic Performance Report**

**Cycle No. 019**

**Start date: 14/06/2017**

**End date: 11/07/2017**



*Mission  
Performance  
Centre*



**Ref.:** S3MPC.ACR.PR.01-019

**Issue:** 1.0

**Date:** 19/07/2017

**Contract:** 400011836/14/I-LG

<b>Customer:</b> ESA	<b>Document Ref.:</b> S3MPC.ACR.PR.01-019
<b>Contract No.:</b> 4000111836/14/I-LG	<b>Date:</b> 19/07/2017
	<b>Issue:</b> 1.0

<b>Project:</b>	PREPARATION AND OPERATIONS OF THE MISSION PERFORMANCE CENTRE (MPC) FOR THE COPERNICUS SENTINEL-3 MISSION		
<b>Title:</b>	S3-A OLCI Cyclic Performance Report		
<b>Author(s):</b>	OLCI ESLs		
<b>Approved by:</b>	L. Bourg, OLCI ESL Coordinator	<b>Authorized by</b>	Frédéric Rouffi, OPT Technical Performance Manager
<b>Distribution:</b>	ESA, EUMETSAT, S3MPC consortium		
<b>Accepted by ESA</b>	S. Dransfeld, MPC Deputy TO for OPT  P. Féménias, MPC TO		
<b>Filename</b>	S3MPC.ACR.PR.01-019 - i1r0 - OLCI Cyclic Report 019.docx		

#### Disclaimer

The work performed in the frame of this contract is carried out with funding by the European Union. The views expressed herein can in no way be taken to reflect the official opinion of either the European Union or the European Space Agency.







Table of content

**TABLE OF CONTENT** ..... **IV**

**LIST OF FIGURES** ..... **V**

**1 INSTRUMENT MONITORING** ..... **1**

1.1 CCD TEMPERATURES..... 1

1.2 RADIOMETRIC CALIBRATION ..... 2

1.2.1 *Dark Offsets [OLCI-L1B-CV-230]* ..... 4

1.2.2 *Instrument response and degradation modelling [OLCI-L1B-CV-250]*..... 7

1.2.3 *Ageing of nominal diffuser [OLCI-L1B-CV-240]*..... 14

1.2.4 *Updating of calibration ADF [OLCI-L1B-CV-260]* ..... 15

1.2.5 *Radiometric Calibrations for sun azimuth angle dependency and Yaw Manoeuvres for Solar Diffuser on-orbit re-characterization [OLCI-L1B-CV-270 and OLCI-L1B-CV-280]*..... 15

1.3 SPECTRAL CALIBRATION [OLCI-L1B-CV-400]..... 15

1.4 SIGNAL TO NOISE ASSESSMENT [OLCI-L1B-CV-620] ..... 15

1.4.1 *SNR from Radiometric calibration data*..... 15

1.4.2 *SNR from EO data*..... 18

1.5 GEOMETRIC CALIBRATION/VALIDATION ..... 18

**2 OLCI LEVEL 1 PRODUCT VALIDATION** ..... **21**

2.1 [OLCI-L1B-CV-300], [OLCI-L1B-CV-310] – RADIOMETRIC VALIDATION ..... 21

2.1.1 *S3ETRAC Service* ..... 21

2.1.2 *Radiometric validation with DIMITRI* ..... 22

2.1.3 *Radiometric validation with OSCAR* ..... 28

**3 LEVEL 2 LAND PRODUCTS VALIDATION** ..... **30**

3.1 [OLCI-L2LRF-CV-300]..... 30

3.2 [OLCI-L2LRF-CV-410 & OLCI-L2LRF-CV-420] – CLOUD MASKING & SURFACE CLASSIFICATION FOR LAND PRODUCTS 30

3.3 VALIDATION OF INTEGRATED WATER VAPOUR OVER LAND ..... 30

**4 LEVEL 2 WATER PRODUCTS VALIDATION** ..... **31**

4.1 [OLCI-L2-CV-210, OLCI-L2-CV-220] – VICARIOUS CALIBRATION OF THE NIR AND VIS BANDS..... 31

4.2 [OLCI-L2WLR-CV-300, OLCI-L2WLR-CV-310, OLCI-L2WLR-CV-32, OLCI-L2WLR-CV-330, OLCI-L2WLR-CV-340, OLCI-L2WLR-CV-350, OLCI-L2WLR-CV-360 AND OLCI-L2WLR-CV-370] – LEVEL 2 WATER-LEAVING REFLECTANCE PRODUCT VALIDATION..... 31


4.3 [OLCI-L2WLR-CV530] VALIDATION OF AEROSOL PRODUCT..... 38

**5 LEVEL 2 SYN PRODUCTS VALIDATION**..... **39**

5.1 [SYN-L2-CV-100] ..... 39

**6 EVENTS** ..... **40**

**7 APPENDIX A** ..... **41**

	<p><b>Sentinel-3 MPC</b></p> <p><b>S3-A OLCI Cyclic Performance Report</b></p> <p><b>Cycle No. 019</b></p>	<p>Ref.: S3MPC.ACR.PR.01-019</p> <p>Issue: 1.0</p> <p>Date: 19/07/2017</p> <p>Page: v</p>
--	--	---

## List of Figures

Figure 1: long term monitoring of CCD temperatures using minimum value (top), time averaged values (middle), and maximum value (bottom) provided in the annotations of the Radiometric Calibration Level 1 products, for the Shutter frames, all radiometric calibrations so far. ----- 1

Figure 2: Same as Figure 1 for diffuser frames. ----- 2

Figure 3: Sun azimuth angles during acquired Radiometric Calibrations (diffuser frame) on top of nominal yearly cycle (black curve). Diffuser 1 with diamonds, diffuser 2 with crosses, 2016 acquisitions in blue, 2017 in red. ----- 3

Figure 4: Sun geometry during radiometric Calibrations on top of characterization ones (diffuser frame) 3

Figure 5: Dark Offset for band Oa1 (top) and Oa21 (bottom), all radiometric calibrations so far except the first one (orbit 183) for which the instrument was not thermally stable yet. ----- 4

Figure 6: map of periodic noise for the 5 cameras, for band Oa21. X-axis is detector number (East part, from 540 to 740, where the periodic noise occurs), Y-axis is the orbit number. The counts have been corrected from the west detectors mean value (not affected by periodic noise). Periodic noise amplitude is high in camera 2, 3 and 4. It is lower in camera 4 and small in camera 1. ----- 5

Figure 7: Dark Current for band Oa1 (top) and Oa21 (bottom), all radiometric calibrations so far except the first one (orbit 183) for which the instrument was not thermally stable yet. ----- 6

Figure 8: left column: ACT mean on 400 first detectors of Dark Current coefficients for spectral band Oa01 (top) and Oa21 (bottom). Right column: same as left column but for Standard deviation instead of mean. We see an increase of the DC level as a function of time especially for band Oa21. A possible explanation could be the increase of the number of hot pixels which is more important in Oa21 because this band is made of more CCD lines than band Oa01 and thus receives more cosmic rays impacts. It is known that cosmic rays degrade the structure of the CCD, generating more and more hot pixels at long term scales. ----- 6

Figure 9: Gain Coefficients for band Oa1 (top) and Oa21 (bottom), all diffuser 1 radiometric calibrations so far except the first one (orbit 183) for which the instrument was not thermally stable yet. ----- 7

Figure 10: camera averaged gain relative evolution with respect to “best geometry” calibration (22/11), as a function of elapsed time since launch; one curve for each band (see colour code on plots), one plot for each module. The star tracker anomaly fix (6/04/16) is represented by a vertical red dashed line. ---- 8

Figure 11: Camera-averaged instrument evolution since channel programming change (25/04/2016) and up to most recent calibration (06/07/2017) versus wavelength. ----- 9

Figure 12: For the 5 cameras: Evolution model performance, as camera-average and standard deviation of ratio of Model over Data vs. wavelength, for each orbit of the test dataset, including 8 calibration in extrapolation, with a colour code for each calibration from blue (oldest) to red (most recent).-----10

Figure 13: model performance: ratio of model over data for all pixels (x axis) of all orbits (y axis), for channel Oa4. The outlying orbit #40 is that of 31/03/2017. -----11


	<b>Sentinel-3 MPC</b> <b>S3-A OLCI Cyclic Performance Report</b> <b>Cycle No. 019</b>	Ref.: S3MPC.ACR.PR.01-019 Issue: 1.0 Date: 19/07/2017 Page: vi
--	---	---

Figure 14: Evolution model performance, as ratio of Model over Data vs. pixels, all cameras side by side, over the whole current calibration dataset (since instrument programming update), including 8 calibration in extrapolation, channels Oa1 to Oa6. -----12

Figure 15: same as Figure 14 for channels Oa7 to Oa14. -----13

Figure 16: same as Figure 14 for channels Oa15 to Oa21.-----14

Figure 17: Signal to Noise ratio as a function of the spectral band for the 5 cameras. These results have been computed from radiometric calibration data. All calibrations except first one (orbit 183) are presents with the colours corresponding to the orbit number (see legend). The SNR is very stable with time: the curves for all orbits are almost superimposed. The dashed curve is the ESA requirement. ----16

Figure 18: long-term stability of the SNR estimates from Calibration data, example of channel Oa1. ----17

Figure 19: histograms of geolocation errors for the along-track (left) and across-track (right) directions.19

Figure 20: georeferencing error in along-track (left) and across-track (right) directions for all the GCPs. 19

Figure 21: average and dispersion time series of the geolocation errors in along-track (blue) and across-track (red) directions over 11 months. -----20

Figure 22: summary of S3ETRAC products generation for OLCI (number of OLCI L1 products Ingested, yellow – number of S3ETRAC extracted products generated, blue – number of S3ETRAC runs without generation of output product (data not meeting selection requirements), green – number of runs ending in error, red, one plot per site type). -----22

Figure 23: Time-series of the elementary ratios (observed/simulated) signal from S3A/OLCI for (top to bottom) bands Oa03, Oa8 and Oa17 respectively over Six PICS Cal/Val sites. Dashed-green and orange lines indicate the 2% and 5% respectively. Error bars indicate the desert methodology uncertainty. ----24

Figure 24: The estimated gain values for S3A/OLCI over the 6 PICS sites identified by CEOS over the period April 2016 – July 2017 as a function of wavelength. Dashed-green and orange lines indicate the 2% and 5% respectively. Error bars indicate the desert methodology uncertainty. -----25

Figure 25: Time-series of the elementary ratios (observed/simulated) signal from (black)S2A/MSI and (blue) S3A/OLCI and (Cyan) Aqua/MODIS for (top) band Oa17: 865nm and (bottom) band Oa08: 665 nm over Mauritania-1 site. Dashed-green and orange lines indicate the 2% and 5% respectively. Error bars indicate the desert methodology uncertainty. -----26

Figure 26: The estimated gain values for S3A/OLCI over the 6 Ocean CalVal sites (Atl-NW\_Optimum, Atl-SW\_Optimum, Pac-NE\_Optimum, Pac-NW\_Optimum, SPG\_Optimum and SIO\_Optimum) over the period December 2016 – July 2017 as a function of wavelength. Dashed-green, and orange lines indicate the 2%, 5% respectively. Error bars indicate the methodology uncertainty. -----27

Figure 27: The estimated gain values for S3A/OLCI from Glint, Rayleigh, and PICS over the period November 2016 – June 2017 as a function of wavelength. We use the gain value of Oa8 from Desert method as reference gain for Glint. Dashed-green and orange lines indicate the 2% and 5% respectively. Error bars indicate the methods uncertainties. -----28

Figure 28: OSCAR Rayleigh results for April 2017-----29


	<p><b>Sentinel-3 MPC</b></p> <p><b>S3-A OLCI Cyclic Performance Report</b></p> <p><b>Cycle No. 019</b></p>	<p>Ref.: S3MPC.ACR.PR.01-019</p> <p>Issue: 1.0</p> <p>Date: 19/07/2017</p> <p>Page: vii</p>
--	--	---

Figure 29: OSCAR Libya-4 deserts results over the period March 2017 –June 2017 in function of wavelength. Only observations with VZA less than 30° are considered. The error bars indicate the standard deviation over the 21 observations.-----29

Figure 30: Scatter plots of OLCI versus in situ radiometry-----34

Figure 31: OLCI and AERONET-OC radiometric time series AAOT station.-----36

Figure 32: OLCI and AERONET-OC radiometric time series Galata station. -----37

Figure 33: OLCI overpath of Galata station (20170612). Chl-NN top left, CHL\_OC4Me, top right, reflectance at 490nm bottom left, TSM-NN bottom right-----38



# 1 Instrument monitoring

## 1.1 CCD temperatures

The monitoring of the CCD temperatures is based on MPMF data extractions not yet operational. In the meantime, we monitor the CCD temperatures on the long-term using Radiometric Calibration Annotations (see Figure 1). Variations are very small (0.09 C peak-to-peak) and no trend can be identified. Data from current cycle (rightmost data points) do not show any specificity.

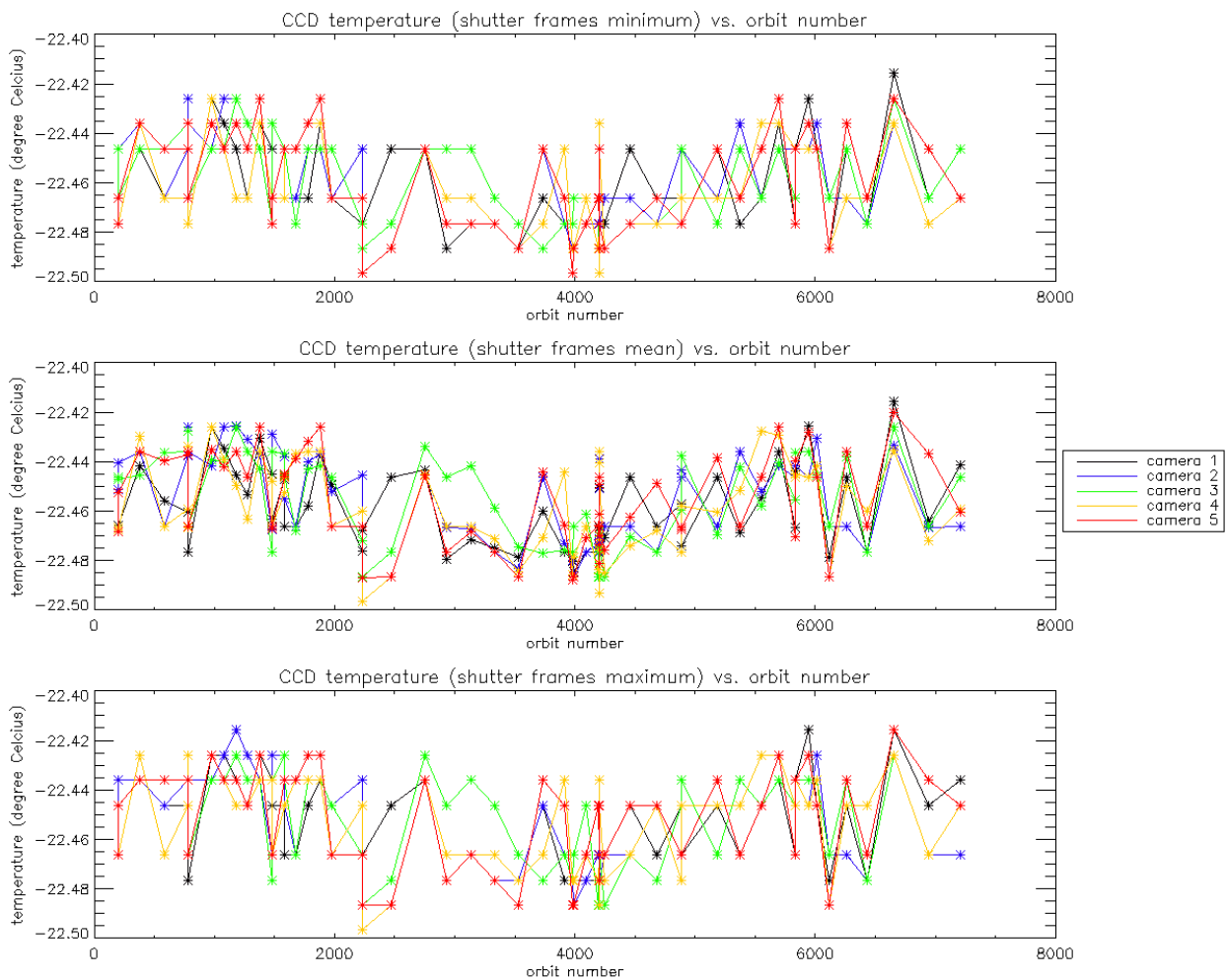


**Figure 1: long term monitoring of CCD temperatures using minimum value (top), time averaged values (middle), and maximum value (bottom) provided in the annotations of the Radiometric Calibration Level 1 products, for the Shutter frames, all radiometric calibrations so far.**



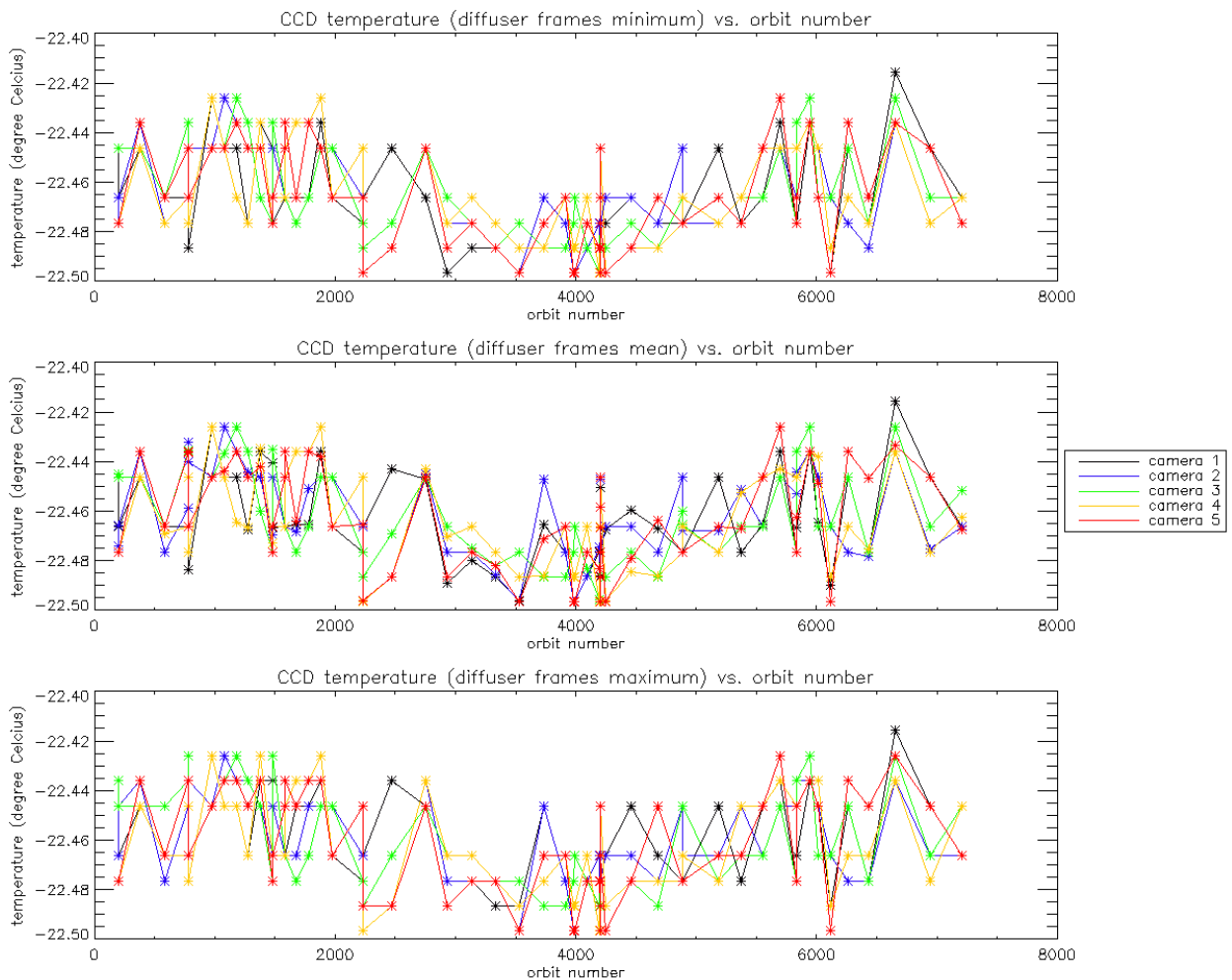


Figure 2: Same as Figure 1 for diffuser frames.

## 1.2 Radiometric Calibration

Two OLCI Radiometric Calibration Sequences have been acquired during Cycle 019:

- ❖ S01 sequence on 17/06/2017 14:59 to 15:01 (absolute orbit 6942)
- ❖ S01 sequence on 06/07/2017 06:42 to 06:44 (absolute orbit 7208)

The acquired Sun azimuth angles are presented on below, on top of the nominal values without Yaw Manoeuvre (i.e. with nominal Yaw Steering control of the satellite).

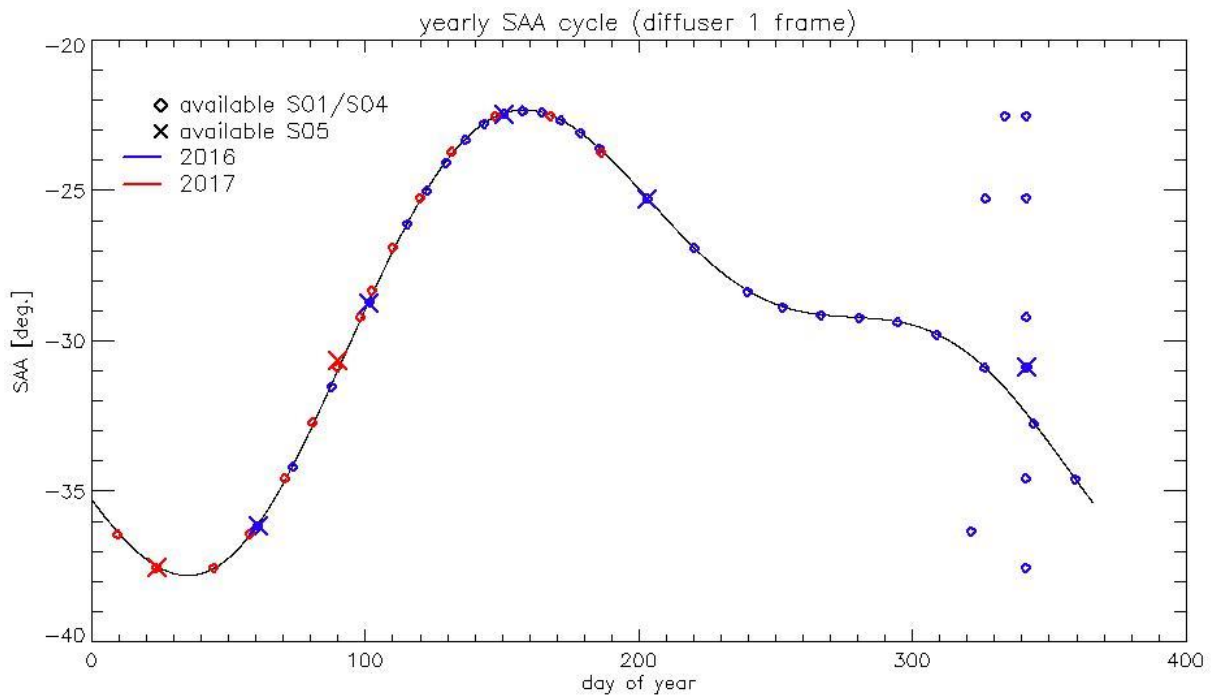


**Figure 3: Sun azimuth angles during acquired Radiometric Calibrations (diffuser frame) on top of nominal yearly cycle (black curve). Diffuser 1 with diamonds, diffuser 2 with crosses, 2016 acquisitions in blue, 2017 in red.**

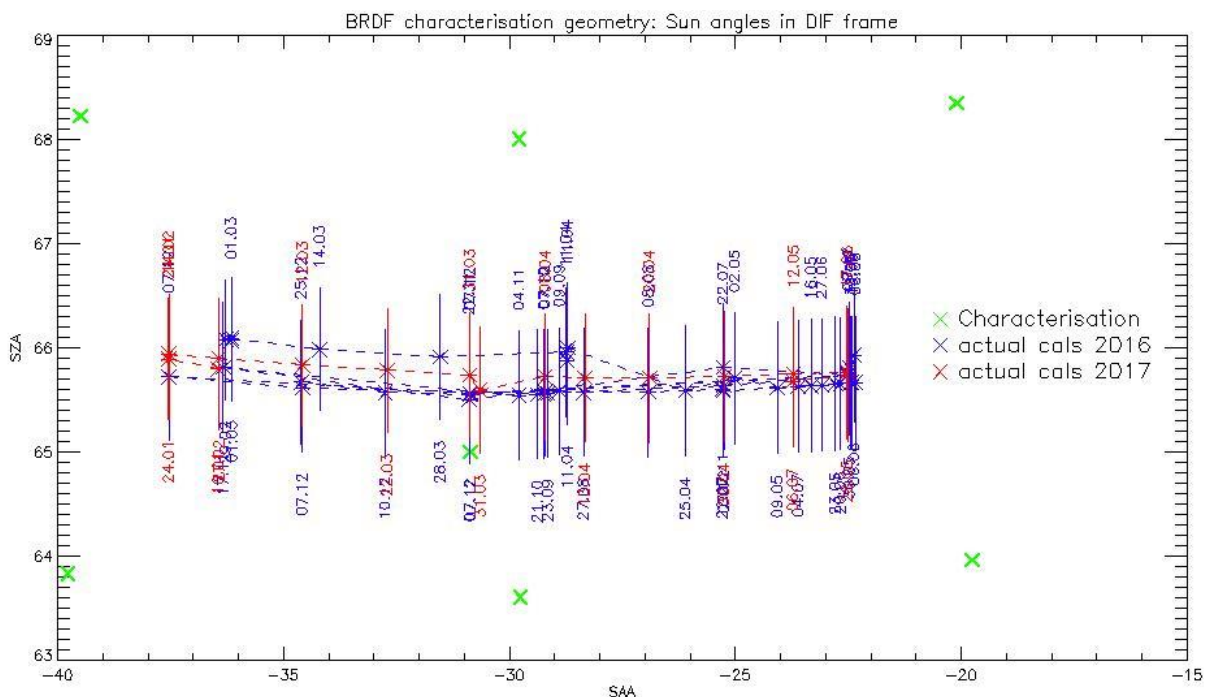


**Figure 4: Sun geometry during radiometric Calibrations on top of characterization ones (diffuser frame)**

This section presents the overall monitoring of the parameters derived from radiometric calibration data and highlights, if present, specificity of current cycle data.



### 1.2.1 Dark Offsets [OLCI-L1B-CV-230]

#### Dark offsets

Dark offsets are continuously affected by the global offset induced by the Periodic Noise on the OLCI convergence. Current Cycle calibrations are affected the same way as others. The amplitude of the shift varies with band and camera from virtually nothing (e.g. camera 2, band Oa1) to up to 5 counts (Oa21, camera 3). The Periodic Noise itself comes on top of the global shift with its known signature: high frequency oscillations with a rapid damp. This effect remains more or less stable with time in terms of amplitude, frequency and decay length, but its phase varies with time, introducing the global offset mentioned above.

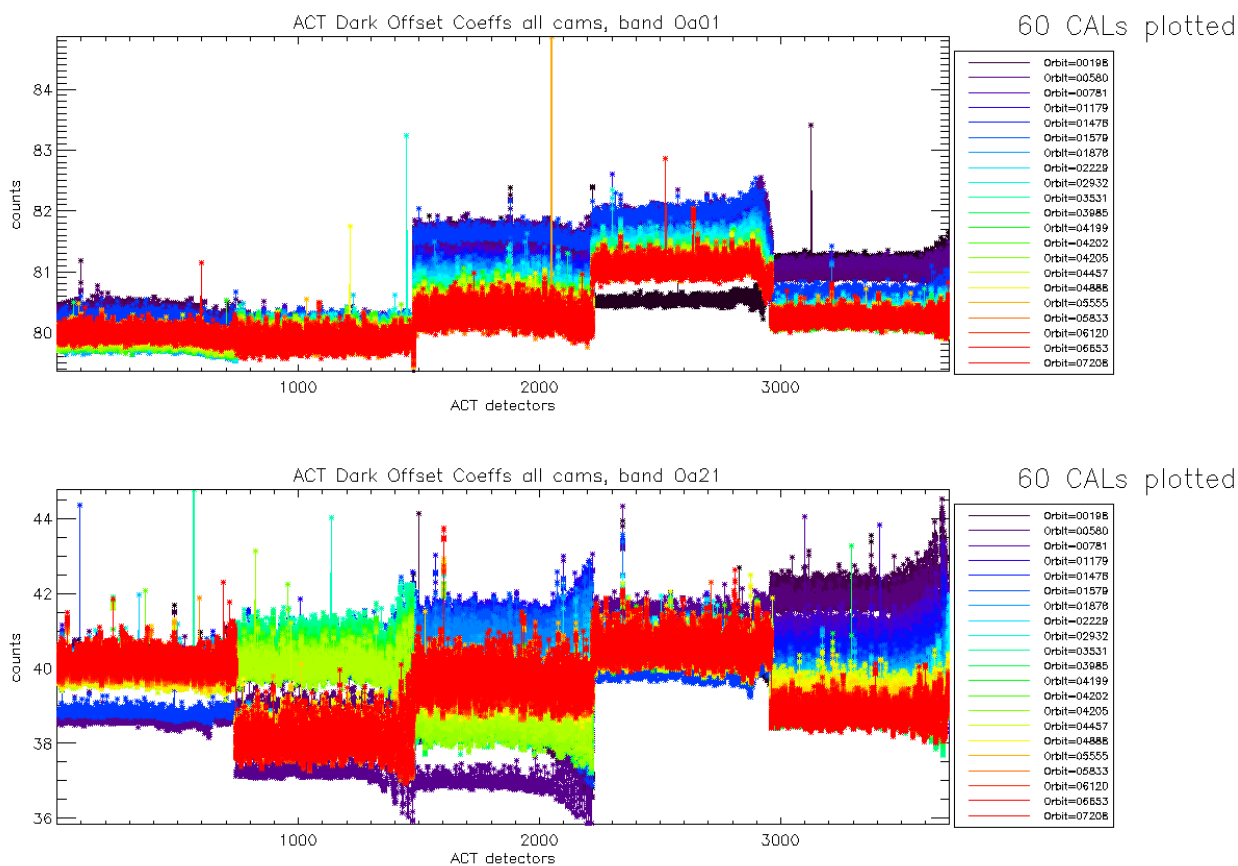


**Figure 5: Dark Offset for band Oa1 (top) and Oa21 (bottom), all radiometric calibrations so far except the first one (orbit 183) for which the instrument was not thermally stable yet.**

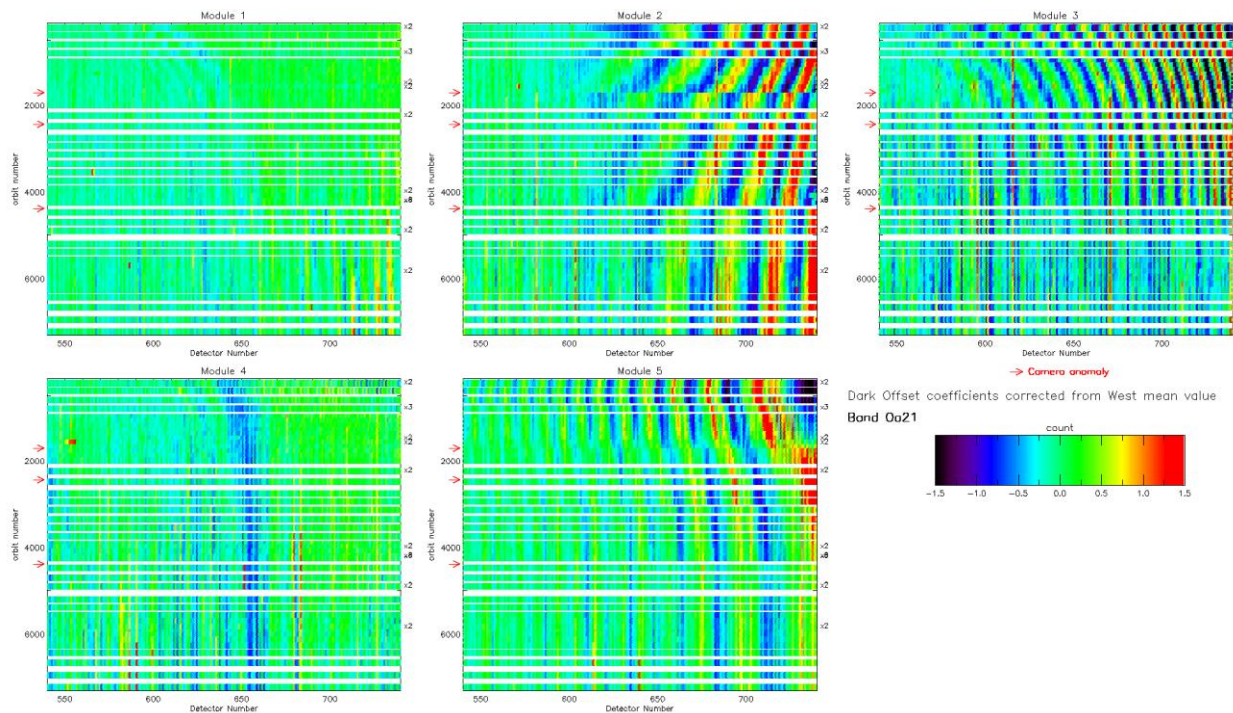


**Figure 6: map of periodic noise for the 5 cameras, for band Oa21. X-axis is detector number (East part, from 540 to 740, where the periodic noise occurs), Y-axis is the orbit number. The counts have been corrected from the west detectors mean value (not affected by periodic noise). Periodic noise amplitude is high in camera 2, 3 and 4. It is lower in camera 4 and small in camera 1.**

Looking at Figure 5 shows no significant evolution of this parameter during the current cycle. Figure 6 shows that since the last sudden PN change (phase and amplitude) caused by the camera-2 anomaly at orbit 4364 (18 December 2016), PN is nearly stabilized again. (See in particular cameras 2, 3 & 5).

### Dark Currents

Dark Currents are not affected by the global offset of the Dark Offsets, thanks to the clamping to the average blind pixels value. However, the oscillations of Periodic Noise remain visible. There is no significant evolution of this parameter during the current cycle.

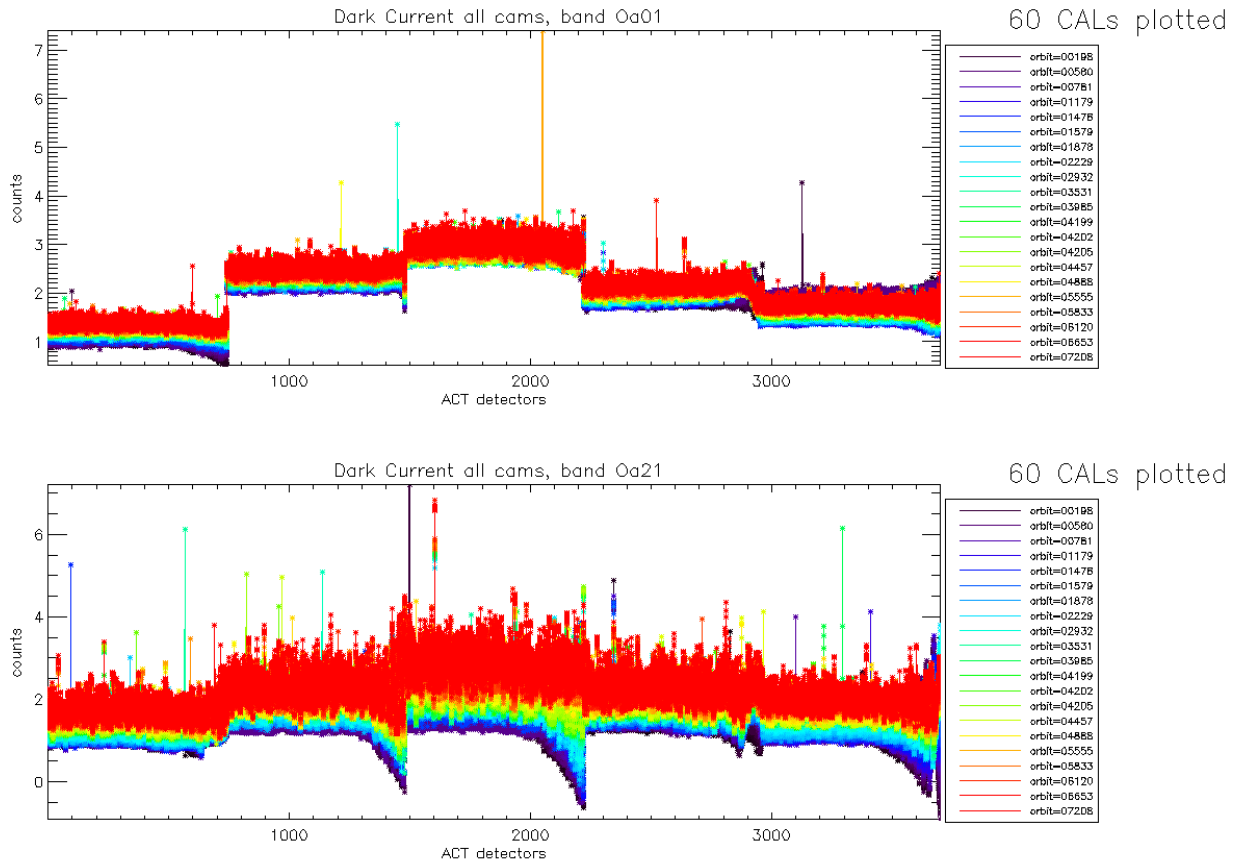


**Figure 7: Dark Current for band Oa1 (top) and Oa21 (bottom), all radiometric calibrations so far except the first one (orbit 183) for which the instrument was not thermally stable yet.**

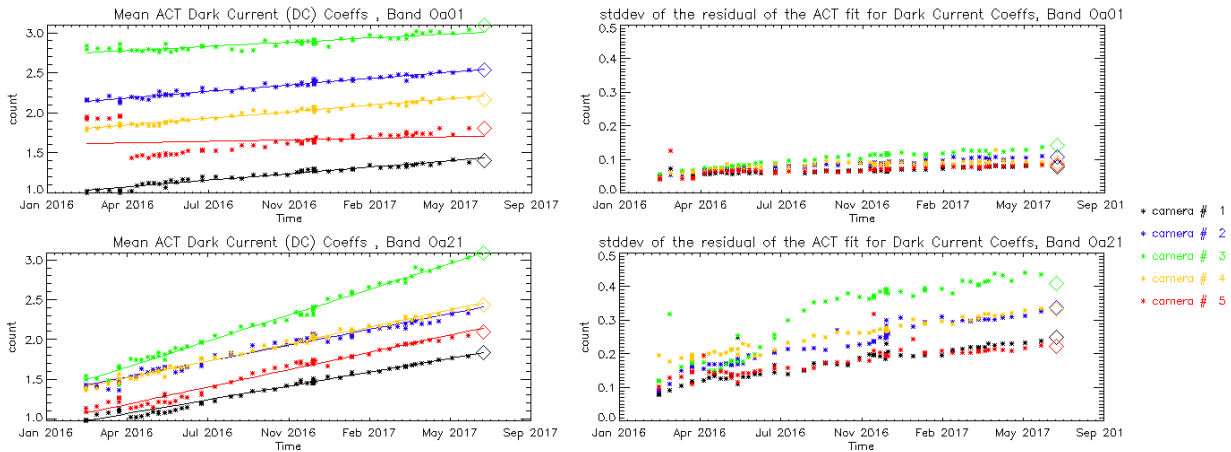


**Figure 8: left column: ACT mean on 400 first detectors of Dark Current coefficients for spectral band Oa01 (top) and Oa21 (bottom). Right column: same as left column but for Standard deviation instead of mean. We see an increase of the DC level as a function of time especially for band Oa21. A possible explanation could be the increase of the number of hot pixels which is more important in Oa21 because this band is made of more CCD lines than band Oa01 and thus receives more cosmic rays impacts. It is known that cosmic rays degrade the structure of the CCD, generating more and more hot pixels at long term scales.**



## 1.2.2 Instrument response and degradation modelling [OLCI-L1B-CV-250]

### 1.2.2.1 Instrument response monitoring

Figure 9 below shows the gain coefficients of every pixel for two OLCI channels, Oa1 (400 nm) and Oa21 (1020 nm), highlighting the significant evolution of the instrument response since early mission.

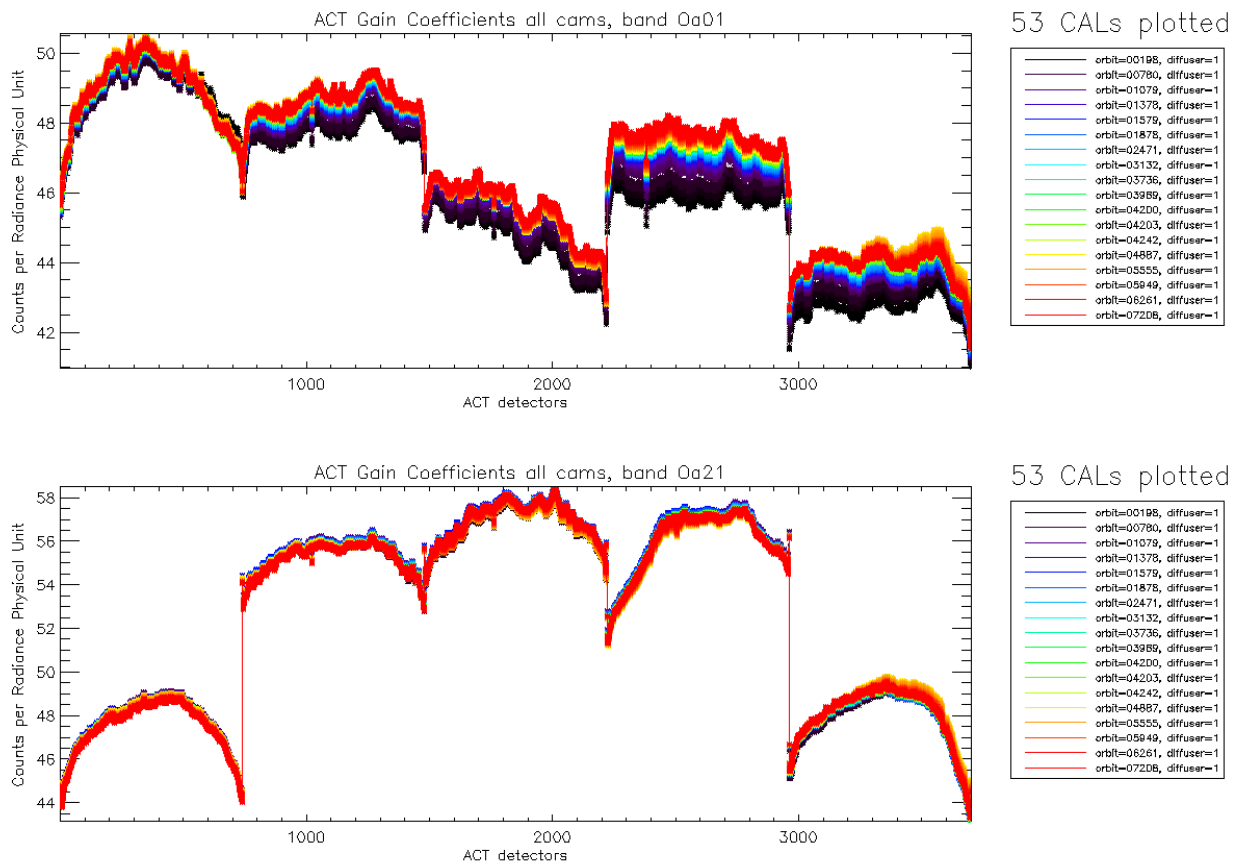


**Figure 9: Gain Coefficients for band Oa1 (top) and Oa21 (bottom), all diffuser 1 radiometric calibrations so far except the first one (orbit 183) for which the instrument was not thermally stable yet.**

The gains plotted in Figure 9, however are derived using the ground BRDF model – as the only one available in the operational processing software so far – which is known to suffer from illumination geometry dependent residual errors (see previous Cyclic Reports for more details). Consequently they are post-processed to replace the ground BRDF model by the in-flight version, based on Yaw Manoeuvres data, prior to determine the radiometric evolution.

Figure 10 displays a summary of the time evolution derived from post-processed gains: the cross-track average of the BRDF corrected gains is plotted as a function of time, for each module, relative to a given reference calibration (the 12/12/2016). It shows that, if a significant evolution occurred during the early mission, the trends tend to stabilize, with the exception of band 1 of camera 4.

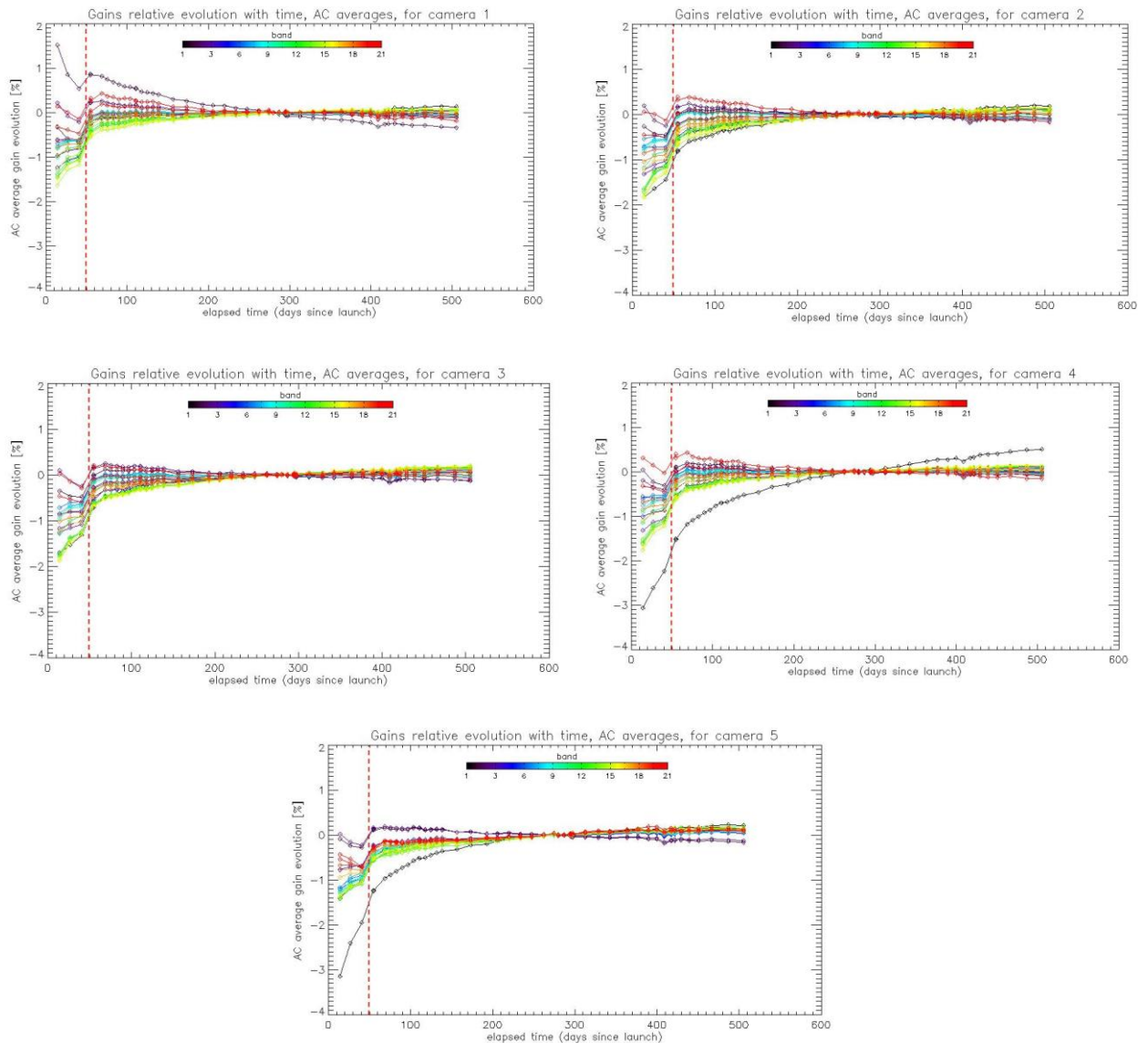


**Figure 10: camera averaged gain relative evolution with respect to “best geometry” calibration (22/11), as a function of elapsed time since launch; one curve for each band (see colour code on plots), one plot for each module. The star tracker anomaly fix (6/04/16) is represented by a vertical red dashed line.**

The behaviour over the first two months of mission, really different and highlighted by Figure 10, is explained by the Star Tracker software anomaly during which the attitude information provided by the platform was corrupted, preventing to compute a correct illumination geometry, with a significant impact on the gain computation.

### 1.2.2.2 Instrument evolution modelling

Thanks to the work done on the Yaw Manoeuvres Calibration acquisitions (see section 1.2.5) an upgraded diffuser BRDF model has been derived, allowing to get rid of the operational model dependency with Sun azimuth discussed above. This in turn allowed building a global gain database

corrected for BRDF error residuals. This database was used as the basis for the derivation of a long-term radiometric drift model.

This required a number of adaptations of the dedicated software for several reasons:

- 1) The upgraded BRDF model is not implemented in the Calibration processing software (IPF OL1-RC), thus the derived gains have to be corrected for BRDF in a post-processing step, on the (justified) assumption that the BRDF changes have a second order impact on the stray-light computation.
- 2) The observed instrument evolution does not follow the expected behaviour: a slow and smooth instrument sensitivity decrease, but on the contrary can show increase as well (see Figure 11))
- 3) The time period is not long enough to correctly model the evolution for cameras/channels for which it is very small: in this case the signal to noise ratio (e. g. due to diffuser speckle) is not high enough and the fit parameters that provide the best match are not physical. As a consequence, it may happen that, despite the model matches very well to the data, its use in extrapolation generates huge drifts that are very unlikely to occur. A post-processing is thus necessary to identify and update those cases.

The model has been derived from the dataset ranging from 26/04/2016 to 12/03/2017, so that the validation dataset now includes 8 calibrations over 2.5 months for performance estimation, including the calibrations acquired during current cycle.

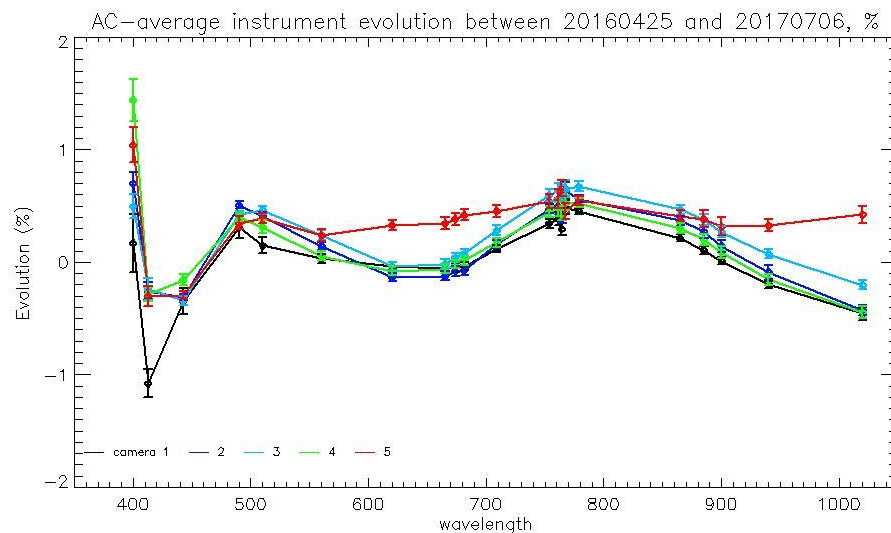


**Figure 11: Camera-averaged instrument evolution since channel programming change (25/04/2016) and up to most recent calibration (06/07/2017) versus wavelength.**

Once these steps are completed, the model performance over the complete dataset (including 8 calibrations in extrapolation over up to 2.5 months) is better than 0.2% except at very specific cases: few isolated pixels in about half of the bands, and two specific features in camera 5 for channels Oa8 and Oa21 that cannot be fitted with a bounded exponential model. The overall performance at each orbit is





shown on Figure 12 as the average and standard deviation of the model over data ratio as a function of wavelength, for each orbit in order to highlight a possible extrapolation issue. If the figure shows an outlying orbit, it must be stressed that it is NOT the most recent, excluding a systematic drift in extrapolation, as proved by Figure 13.

Finally, Figure 14 to Figure 16 show the detail of the model performance, with across-track plots of the model over data ratios at each orbit, one plot for each channel.

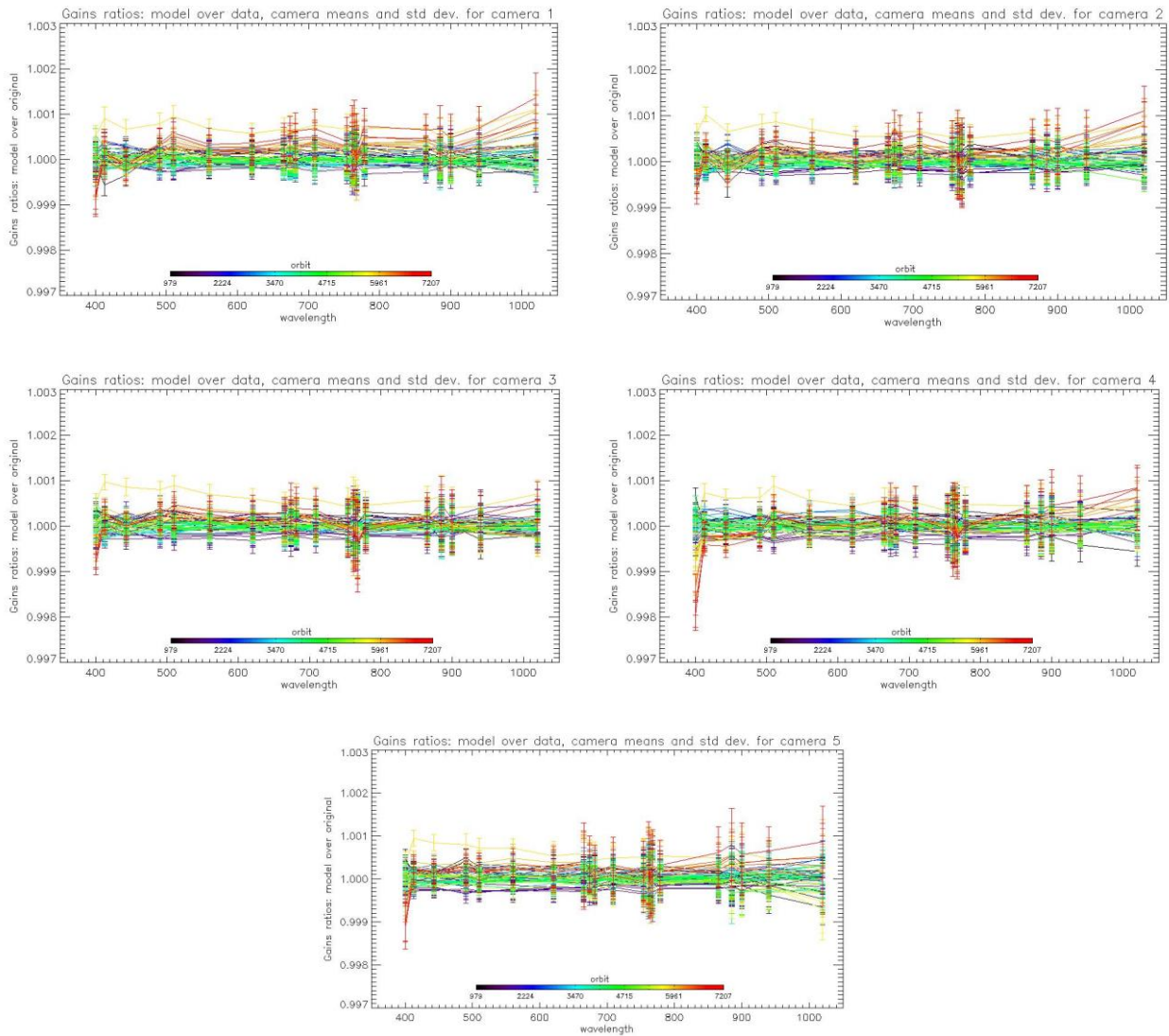


**Figure 12: For the 5 cameras: Evolution model performance, as camera-average and standard deviation of ratio of Model over Data vs. wavelength, for each orbit of the test dataset, including 8 calibration in extrapolation, with a colour code for each calibration from blue (oldest) to red (most recent).**

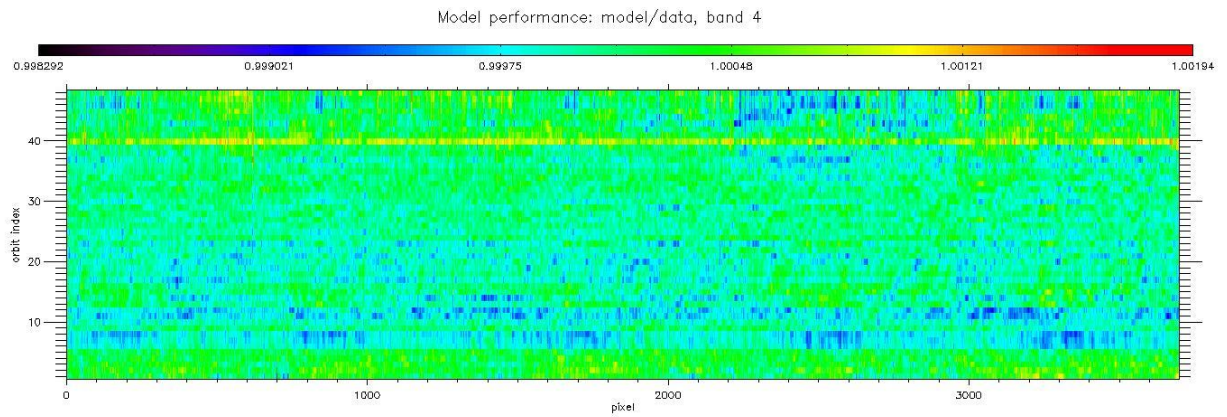


**Figure 13: model performance: ratio of model over data for all pixels (x axis) of all orbits (y axis), for channel Oa4. The outlying orbit #40 is that of 31/03/2017.**

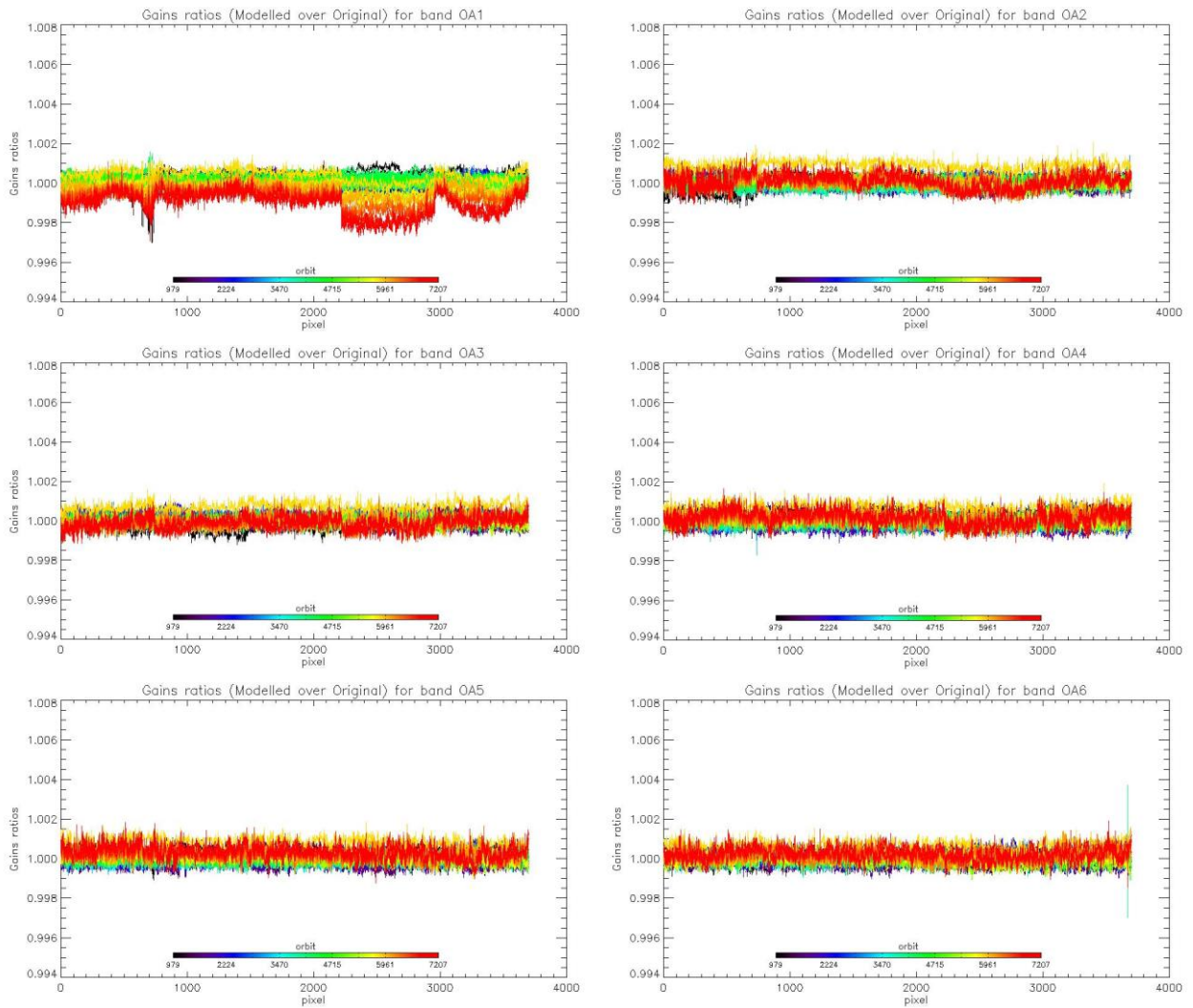


**Figure 14: Evolution model performance, as ratio of Model over Data vs. pixels, all cameras side by side, over the whole current calibration dataset (since instrument programming update), including 8 calibration in extrapolation, channels Oa1 to Oa6.**



Sentinel-3 MPC  
S3-A OLCI Cyclic Performance Report  
Cycle No. 019

Ref.: S3MPC.ACR.PR.01-019  
Issue: 1.0  
Date: 19/07/2017  
Page: 13

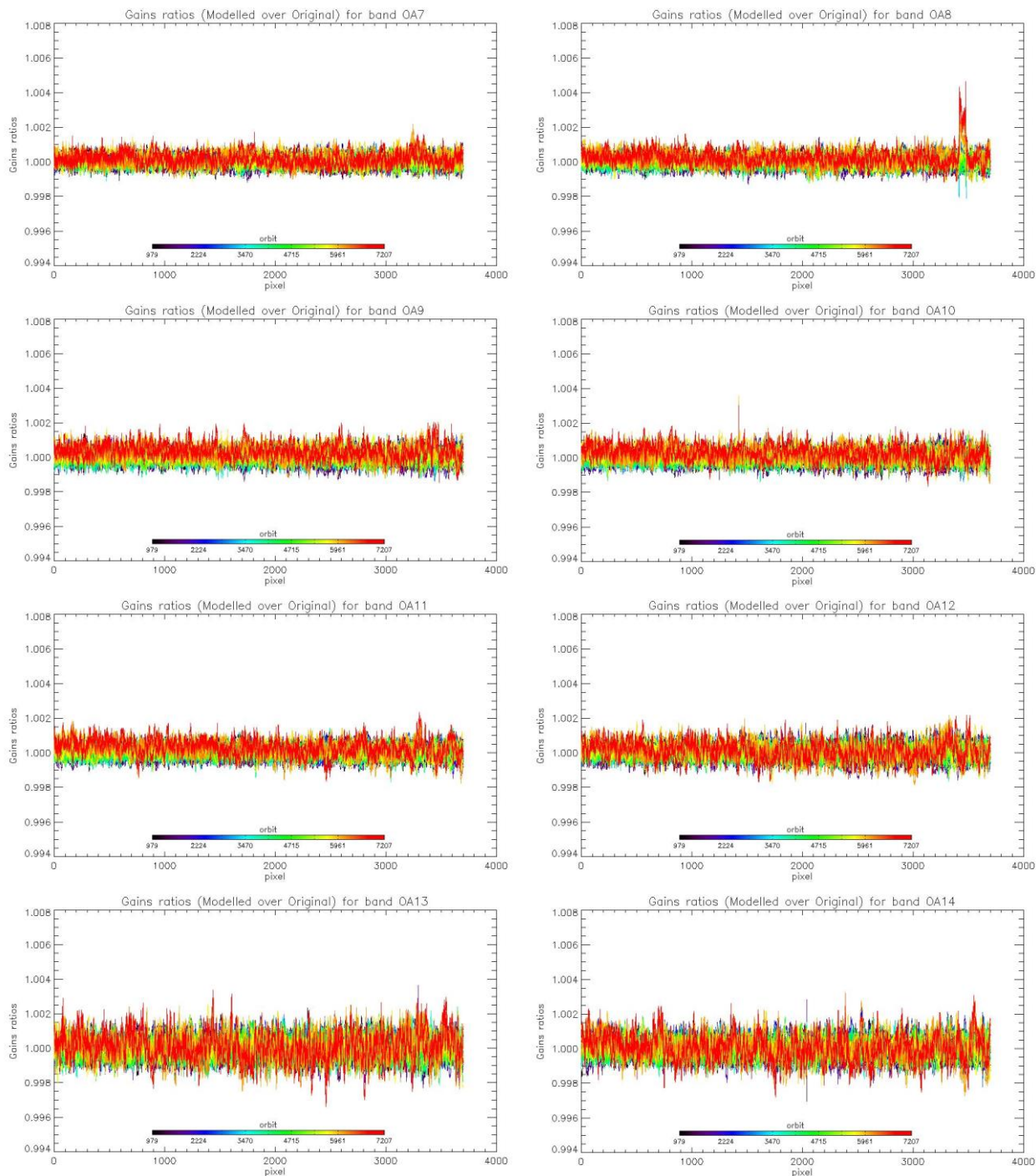


Figure 15: same as Figure 14 for channels Oa7 to Oa14.



Sentinel-3 MPC  
S3-A OLCI Cyclic Performance Report  
Cycle No. 019

Ref.: S3MPC.ACR.PR.01-019  
Issue: 1.0  
Date: 19/07/2017  
Page: 14

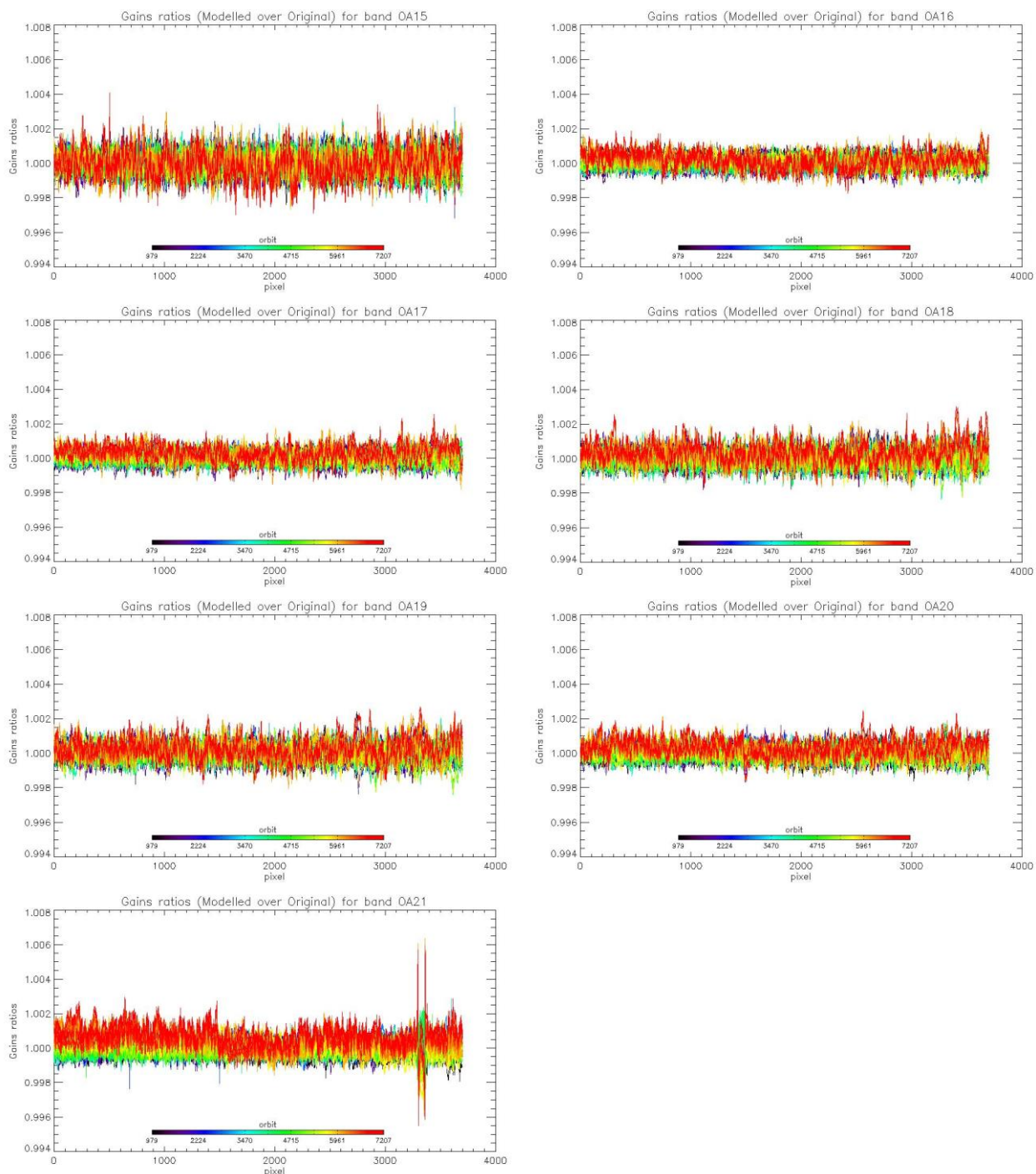



Figure 16: same as Figure 14 for channels Oa15 to Oa21.

### 1.2.3 Ageing of nominal diffuser [OLCI-L1B-CV-240]

There has been no calibration sequence S05 (reference diffuser) acquisition during cycle 019.

Consequently the last updated results (cycle 016) are still valid.

	<b>Sentinel-3 MPC</b> <b>S3-A OLCI Cyclic Performance Report</b> <b>Cycle No. 019</b>	Ref.: S3MPC.ACR.PR.01-019 Issue: 1.0 Date: 19/07/2017 Page: 15
--	---	---

#### 1.2.4 Updating of calibration ADF [OLCI-L1B-CV-260]

There has been no OL\_1\_CAL\_AX generated during cycle 019.

#### 1.2.5 Radiometric Calibrations for sun azimuth angle dependency and Yaw Manoeuvres for Solar Diffuser on-orbit re-characterization [OLCI-L1B-CV-270 and OLCI-L1B-CV-280]

This activity has not evolved during cycle 019 and results presented in previous report are still valid.

### 1.3 Spectral Calibration [OLCI-L1B-CV-400]

---

There has been no Spectral Calibration acquisitions sequence S02/S03 during cycle 019.

Consequently the last updated results (cycle 018) are still valid.

### 1.4 Signal to Noise assessment [OLCI-L1B-CV-620]

---

#### 1.4.1 SNR from Radiometric calibration data.

SNR computed for all calibration data as a function of band number is presented in Figure 17.

SNR computed for all calibration data as a function of orbit number for band Oa01 (the less stable band) is presented in Figure 18.

There is no significant evolution of this parameter during the current cycle and the ESA requirement is fulfilled for all bands.

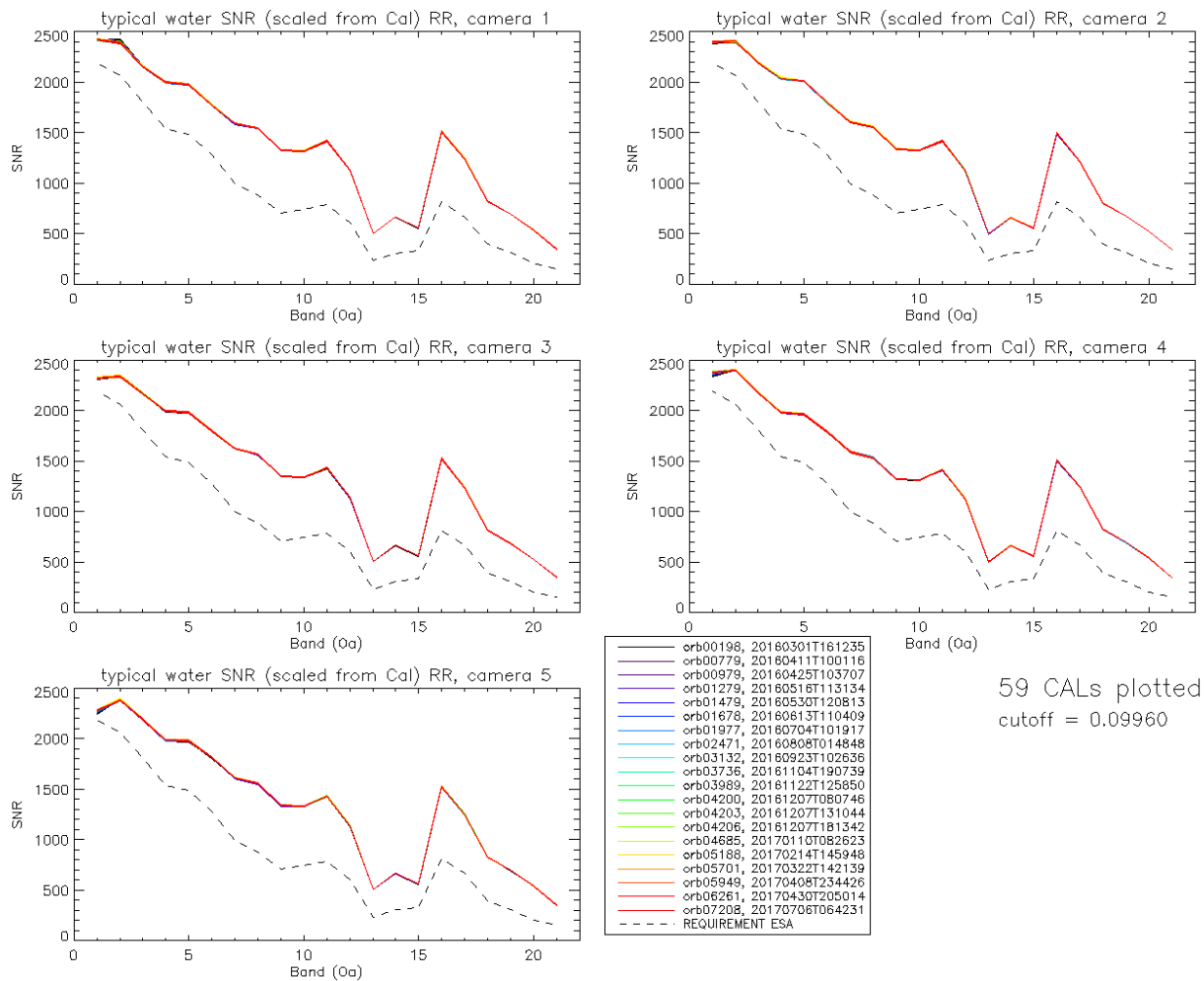


**Figure 17: Signal to Noise ratio as a function of the spectral band for the 5 cameras. These results have been computed from radiometric calibration data. All calibrations except first one (orbit 183) are presents with the colours corresponding to the orbit number (see legend). The SNR is very stable with time: the curves for all orbits are almost superimposed. The dashed curve is the ESA requirement.**

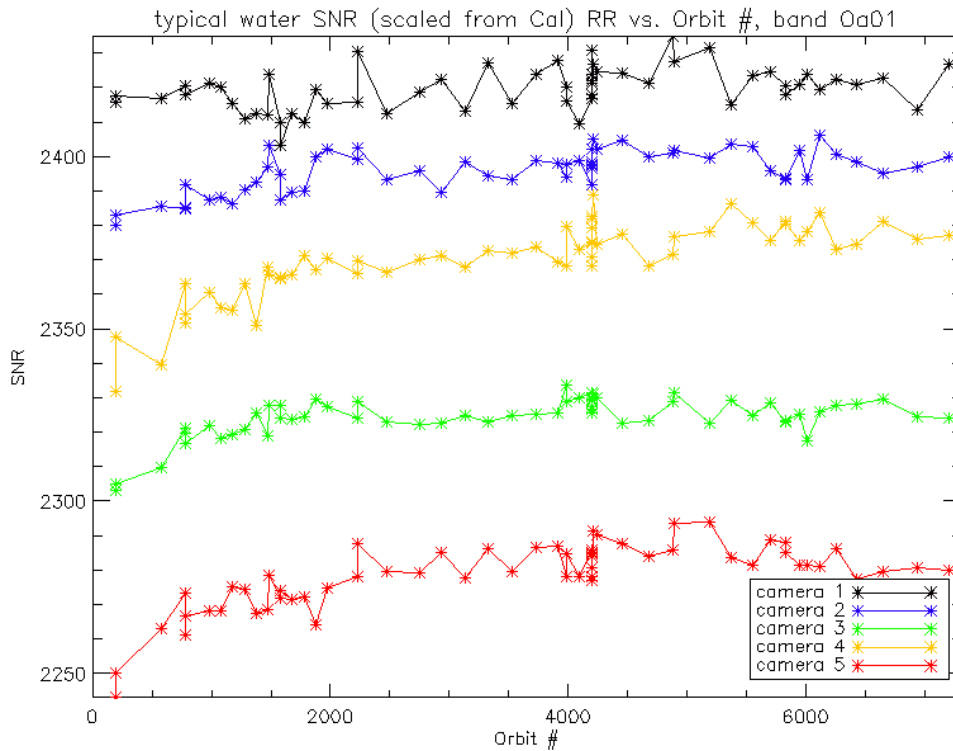


**Figure 18: long-term stability of the SNR estimates from Calibration data, example of channel Oa1.**

The mission averaged SNR figures are provided in Table 1 below, together with their radiance reference level. According to the OLCI SNR requirements, these figures are valid at these radiance levels and at Reduced Resolution (RR, 1.2 km). They can be scaled to other radiance levels assuming shot noise (CCD sensor noise) is the dominating term, i.e. radiometric noise can be considered Gaussian with its standard deviation varying as the square root of the signal; in other words:  $SNR(L) = SNR(L_{ref}) \cdot \sqrt{\frac{L}{L_{ref}}}$ . Following the same assumption, values at Full Resolution (300m) can be derived from RR ones as 4 times smaller.





**Sentinel-3 MPC**  
**S3-A OLCI Cyclic Performance Report**  
**Cycle No. 019**

Ref.: S3MPC.ACR.PR.01-019  
 Issue: 1.0  
 Date: 19/07/2017  
 Page: 18

**Table 1: SNR figures as derived from Radiometric Calibration data. Figures are given for each camera (time average and standard deviation), and for the whole instrument. The requirement and its reference radiance level are recalled (in  $mW.sr^{-1}.m^{-2}.nm^{-1}$ ).**

$\lambda$	$L_{ref}$	SNR	C1		C2		C3		C4		C5		All	
			avg	std	avg	std	avg	std	avg	std	avg	std	avg	std
400	63	2188	2419	6.6	2395	6	2324	6	2369	11	2278	10.1	2357	6.4
412.5	74.1	2061	2397	8.2	2409	5.3	2340	4.9	2402	4.6	2386	7.2	2387	4.1
442.5	65.6	1811	2161	5.5	2200	5.9	2167	4.4	2185	4.3	2197	4.9	2182	3.4
490	51.2	1541	1999	5.1	2035	5.5	1995	3.5	1981	4.1	1987	5.2	1999	3.6
510	44.4	1488	1979	5.6	2012	4.9	1982	4.4	1965	4.6	1984	5	1984	3.9
560	31.5	1280	1775	4.4	1801	4.5	1801	5	1793	4	1817	3.9	1797	3.3
620	21.1	997	1591	4.3	1609	4.3	1625	3.4	1593	3.5	1614	3.8	1606	2.9
665	16.4	883	1546	4.8	1558	4.2	1566	3.8	1532	4.4	1560	4	1552	3.4
673.75	15.7	707	1329	3.5	1338	4.1	1350	2.9	1323	3.1	1341	4.1	1336	2.8
681.25	15.1	745	1319	3.8	1326	3.3	1337	3	1314	2.5	1332	4	1326	2.4
708.75	12.7	785	1420	4.7	1420	4.5	1434	3.7	1413	4	1429	3.2	1423	3.2
753.75	10.3	605	1126	3.5	1119	3.4	1133	3.9	1123	2.8	1137	3	1128	2.8
761.25	6.1	232	501	1.3	498	1.5	504	1.4	500	1.2	507	1.6	502	1.1
764.375	7.1	305	662	1.8	657	1.8	667	2.5	660	1.8	668	2.1	663	1.7
767.5	7.6	330	558	1.9	554	1.3	561	1.6	556	1.8	563	1.5	558	1.4
778.75	9.2	812	1513	5.5	1495	5.4	1522	5.6	1508	5.8	1524	5.3	1513	4.9
865	6.2	666	1243	3.9	1212	4.5	1237	4.5	1245	3.9	1249	3	1237	3.5
885	6	395	823	2	801	1.8	813	2.2	824	1.6	830	2	818	1.5
900	4.7	308	691	1.6	673	1.4	682	1.8	693	1.5	697	1.6	687	1.1
940	2.4	203	534	1	522	1.2	525	1	539	1.2	541	1.2	532	0.8
1020	3.9	152	345	0.8	337	0.7	348	0.8	345	0.7	351	0.7	345	0.5

#### 1.4.2 SNR from EO data.

There has been no update on SNR assessment from EO data during the cycle. Last figures (cycle 9) are considered valid.

### 1.5 Geometric Calibration/Validation

Regular monitoring using the GeoCal Tool implemented within the MPMF continues. Late June results confirm good performance. Monitoring of the geolocation performance by correlation with GCP imageries using the GeoCal tool over the period confirms that OLCI is compliant with its requirement: the centroid of the geolocation error is around 0.25 pixel in both along-track and across-track directions (Figure 19: histograms of geolocation errors for the along-track (left) and across-track (right) directions).

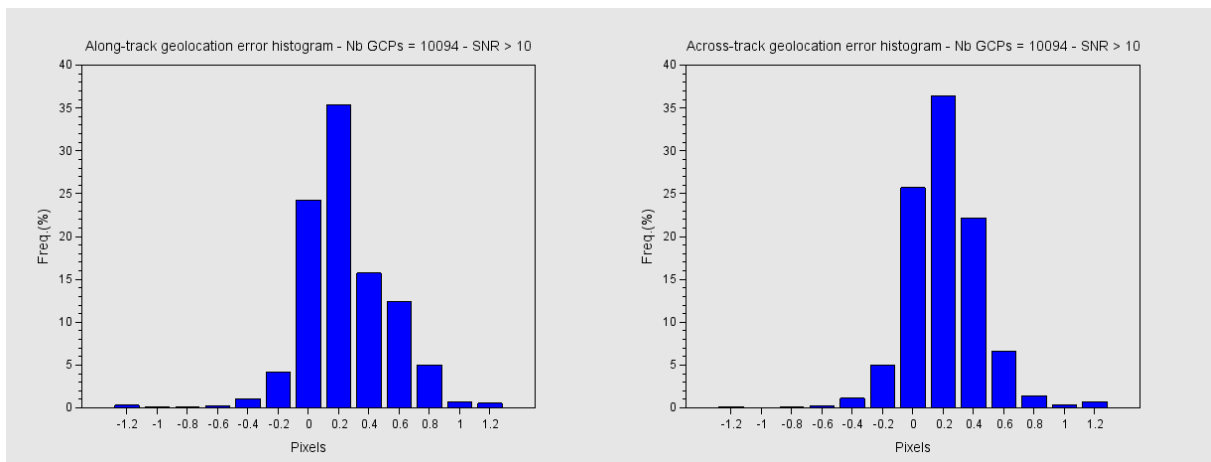


**Figure 19: histograms of geolocation errors for the along-track (left) and across-track (right) directions.**

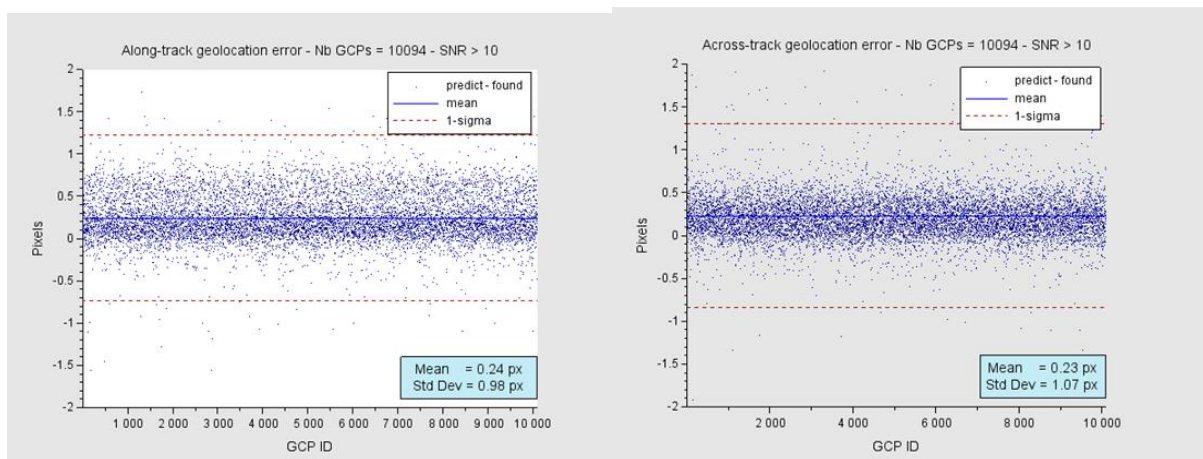


**Figure 20: georeferencing error in along-track (left) and across-track (right) directions for all the GCPs.**

The series plots of along-track and across-track georeferencing errors (Figure 20) show the good overall performance of the geometric calibration but also highlight the significant number of outliers, despite the filtering on correlation level (SNR). This shows that wrong correlations are still present despite the filtering on the internal quality estimator “SNR” and suggest including additional filtering on the error magnitude itself.

Thanks to a partial reprocessing of Level 1 data spread over almost the mission duration (May 2016 to March 2107, 1 day per month), it was possible to generalize the analysis to a large time window and introduce additional filtering to get meaningful dispersion values. This analysis allowed detecting a small but continuous trend in AL average that does not seem to be cyclic and a slight discrete increase of the across-track average error in November 2016 (Figure 21). In-depth analysis, in particular regarding camera and pixel dependencies, as well as potential latitudinal effects, has started.

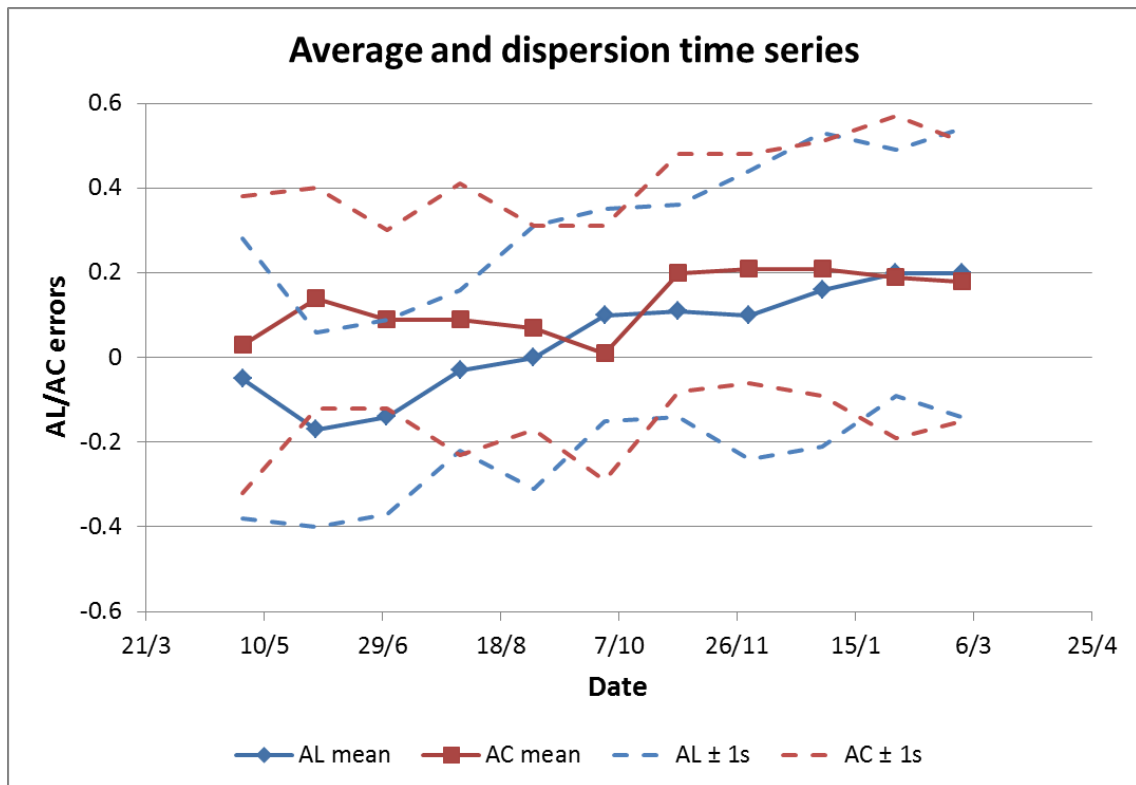



Figure 21: average and dispersion time series of the geolocation errors in along-track (blue) and across-track (red) directions over 11 months.

	<b>Sentinel-3 MPC</b> <b>S3-A OLCI Cyclic Performance Report</b> <b>Cycle No. 019</b>	Ref.: S3MPC.ACR.PR.01-019 Issue: 1.0 Date: 19/07/2017 Page: 21
--	---	---

## 2 OLCI Level 1 Product validation

### 2.1 [OLCI-L1B-CV-300], [OLCI-L1B-CV-310] – Radiometric Validation

---

#### 2.1.1 S3ETRAC Service

##### Activities done

The S3ETRAC service extracts OLCI L1 RR and SLSTR L1 RBT data and computes associated statistics over 49 sites corresponding to different surface types (desert, snow, ocean maximizing Rayleigh signal, ocean maximizing sunglint scattering and deep convective clouds). The S3ETRAC products are used for the assessment and monitoring of the L1 radiometry (optical channels) by the ESLs.

All details about the S3ETRAC/OLCI and S3ETRAC/SLSTR statistics are provided on the S3ETRAC website <http://s3etrac.acri.fr/index.php?action=generalstatistics>

- ❖ Number of OLCI products processed by the S3ETRAC service
- ❖ Statistics per type of target (DESERT, SNOW, RAYLEIGH, SUNGLINT and DCC)
- ❖ Statistics per sites
- ❖ Statistics on the number of records

For illustration, we provide below statistics on the number of S3ETRAC/OLCI records generated per type of targets (DESERT, SNOW, RAYLEIGH, SUNGLINT and DCC).

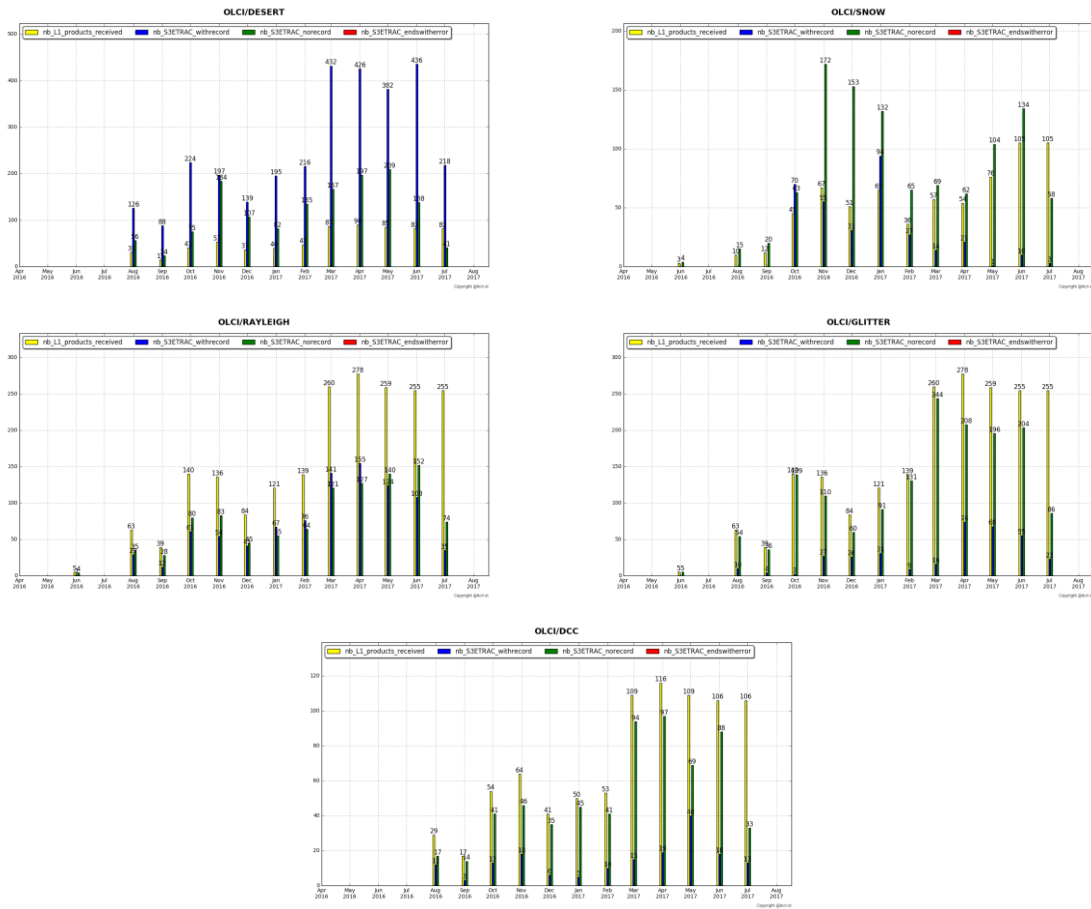



**Figure 22: summary of S3ETRAC products generation for OLCI (number of OLCI L1 products Ingested, yellow – number of S3ETRAC extracted products generated, blue – number of S3ETRAC runs without generation of output product (data not meeting selection requirements), green – number of runs ending in error, red, one plot per site type).**

### 2.1.2 Radiometric validation with DIMITRI

#### Highlights

- ❖ Identified and fixed an issue with OLCI readers in DIMITRI
- ❖ Regenerate all the previous results
- ❖ The results are consistent over the three methods (Rayleigh, Glint and PICS).
- ❖ Rather good stability of the sensor could be seen, nevertheless, the time-series average shows higher reflectance over the VNIR spectral range with bias of 3%-5% except bands Oa07-Oa09; bands with high gaseous absorption are excluded.
- ❖ The results are consistent over the used CalVal sites

	<p><b>Sentinel-3 MPC</b></p> <p><b>S3-A OLCI Cyclic Performance Report</b></p> <p><b>Cycle No. 019</b></p>	<p>Ref.: S3MPC.ACR.PR.01-019</p> <p>Issue: 1.0</p> <p>Date: 19/07/2017</p> <p>Page: 23</p>
--	--	--

- ❖ The results need to be consolidated over ocean sites with more products from early mission period.

### I-Validation over PICS

1. Downloading and ingestion of all the available L1B-LN1-NT products in the S3A-Opt database over the 6 desert calval-sites (Algeria3 & 5, Libya 1 & 4 and Mauritania 1 & 2) is on-going. The ingested time-series has been extended until 17<sup>th</sup> July 2017. Note that only 8 products over the 6 PICS were found during Cycle-19 period, which are not enough to provide a solid analysis.
2. The results are consistent overall the six used PICS sites (Figure 23). OLCI reflectance shows rather good stability over the mission life.
3. The temporal average over the period **April 2016 – July 2017** of the elementary ratios (observed reflectance to the simulated one) shows values higher than 2% (mission requirements) over all the VNIR bands (Figure 24). The spectral bands with significant absorption from water vapor and O<sub>2</sub> (Oa11, Oa13 and Oa14) show an outlier ratio.

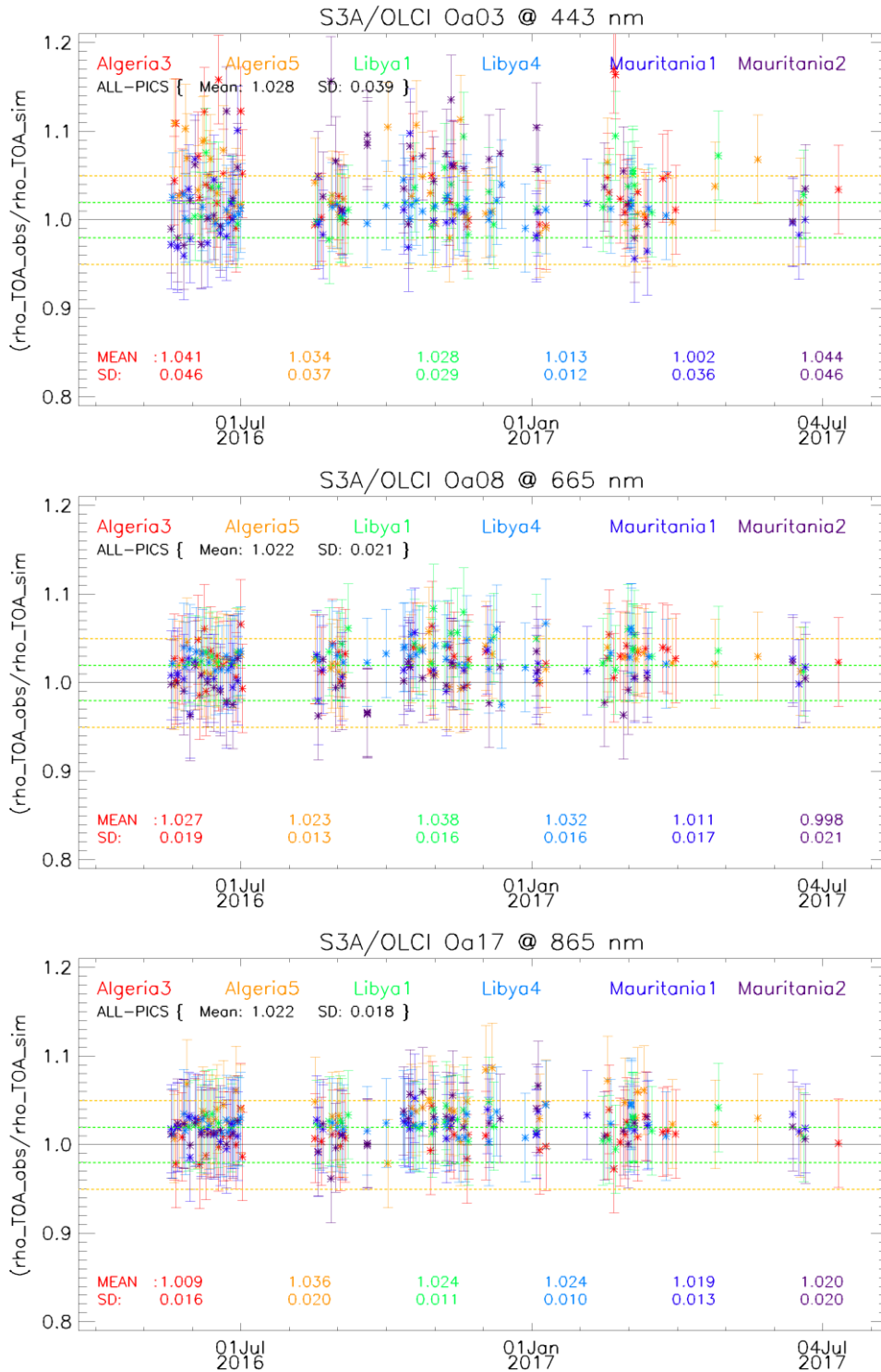


**Figure 23: Time-series of the elementary ratios (observed/simulated) signal from S3A/OLCI for (top to bottom) bands Oa03, Oa08 and Oa17 respectively over Six PICS Cal/Val sites. Dashed-green and orange lines indicate the 2% and 5% respectively. Error bars indicate the desert methodology uncertainty.**

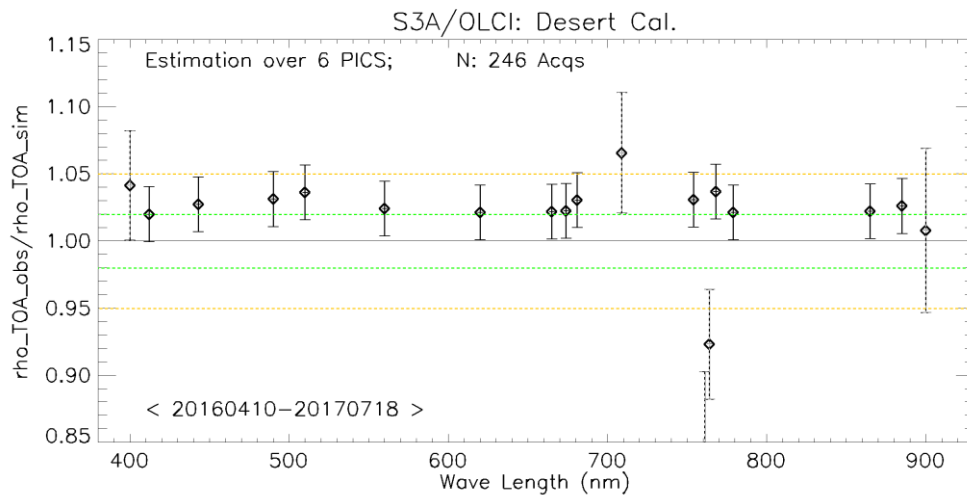


**Figure 24: The estimated gain values for S3A/OLCI over the 6 PICS sites identified by CEOS over the period April 2016 – July 2017 as a function of wavelength. Dashed-green and orange lines indicate the 2% and 5% respectively. Error bars indicate the desert methodology uncertainty.**

## II-Intercomparison S3A/OLCI, S2A/MSI and LANDSAT/OLI over PICS

1. X-mission Intercomparison with MSI-A and MODIS-A is performed until July 2017. Figure 25 shows time-series of the elementary ratios from S2A/MSI, Aqua/MODIS and S3A/OLCI over Mauritania-1 over the period March-2016 until July-2017.

We observe a clear stability over the three sensors, associated with high reflectance from OLCI wrt to MSI and MODIS ones.



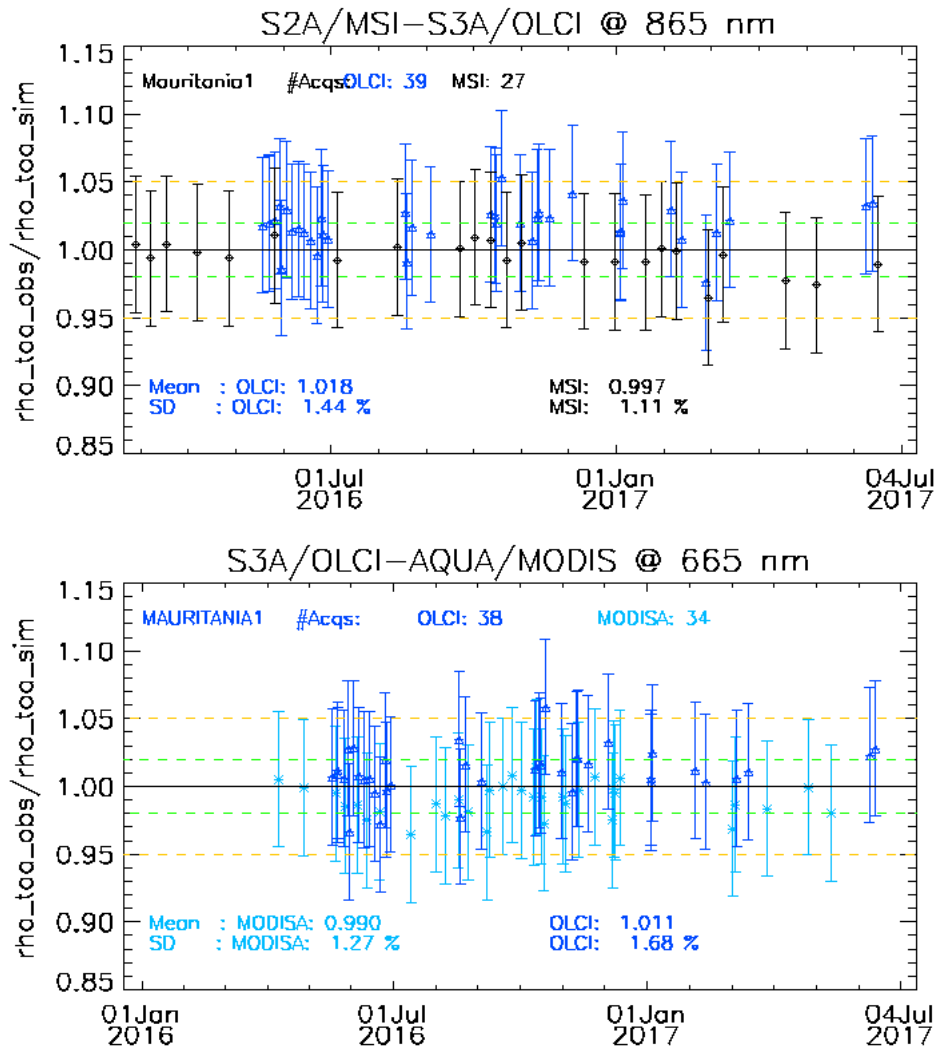


**Figure 25: Time-series of the elementary ratios (observed/simulated) signal from (black)S2A/MSI and (blue) S3A/OLCI and (Cyan) Aqua/MODIS for (top) band Oa17: 865nm and (bottom) band Oa08: 665 nm over Mauritania-1 site. Dashed-green and orange lines indicate the 2% and 5% respectively. Error bars indicate the desert methodology uncertainty.**

### III-Validation over Rayleigh

After the correction of DIMITRI-issue, Rayleigh method has been performed over the available mini-files on the Opt-server over the period December 2016 – July 2017. The results produced with the configuration (ROI-AVERAGE) are consistent with the previous results of PICS method. While bands Oa01-Oa05 display a bias values between 2%-5%, bands Oa6-Oa9 exhibit biases within 2% (mission requirements) (Figure 26).

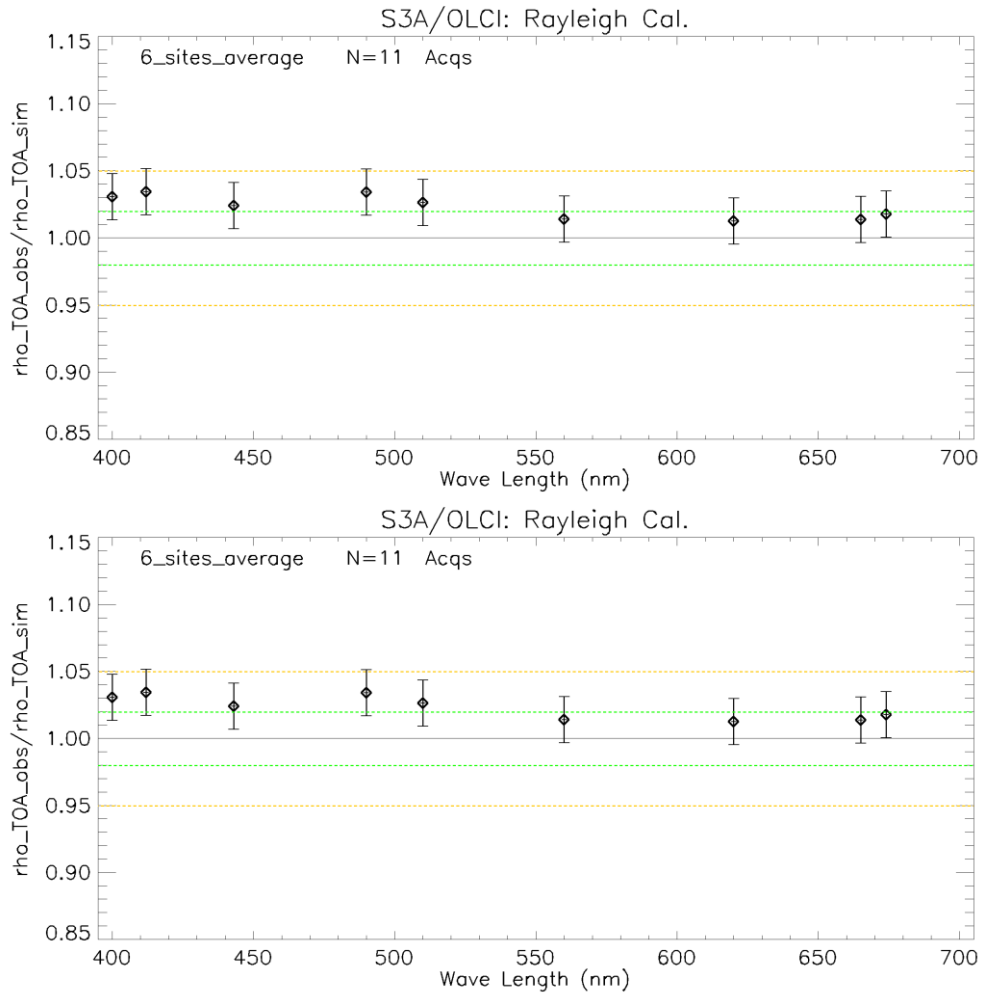


**Figure 26: The estimated gain values for S3A/OLCI over the 6 Ocean CalVal sites (Atl-NW\_Optimum, Atl-SW\_Optimum, Pac-NE\_Optimum, Pac-NW\_Optimum, SPG\_Optimum and SIO\_Optimum) over the period December 2016 – July 2017 as a function of wavelength. Dashed-green, and orange lines indicate the 2%, 5% respectively. Error bars indicate the methodology uncertainty.**

#### IV-Validation over Glint

Glint calibration method with the configuration (ROI-PIXEL) has been performed over the period September 2016 – June 2017 from the available mini-files. The outcome of this analysis shows a good consistency with the desert outputs over the red spectral range (see Figure 27).

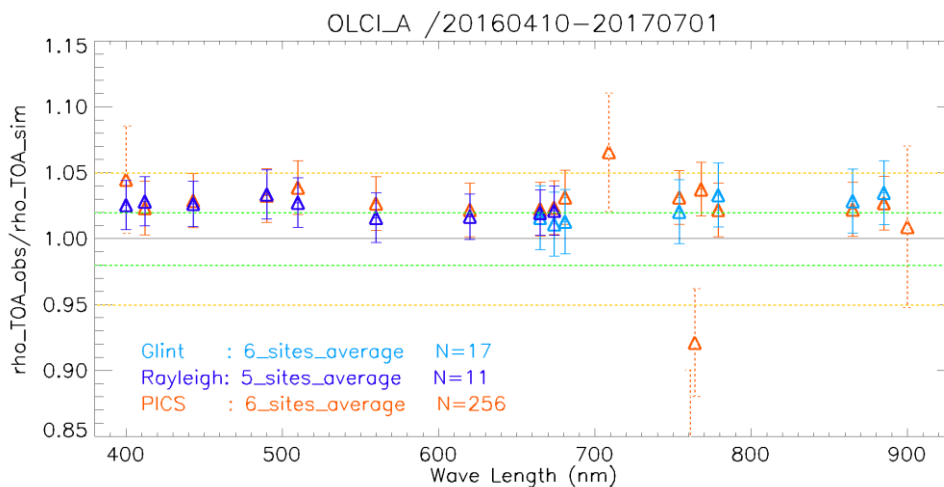


**Figure 27: The estimated gain values for S3A/OLCI from Glint, Rayleigh, and PICS over the period November 2016 – June 2017 as a function of wavelength. We use the gain value of Oa8 from Desert method as reference gain for Glint. Dashed-green and orange lines indicate the 2% and 5% respectively. Error bars indicate the methods uncertainties.**

### 2.1.3 Radiometric validation with OSCAR

To reduce the scattering in the OSCAR Rayleigh results for OLCI an extra quality check has been added based on the airmass. Average results per site for April 2017 are given in Figure 28.

A preliminary verification of the OLCI radiometry is performed on the basis of the Libya-4 OSCAR desert approach (Govaerts, Y., S. Sterckx, and S. Adriaensen (2013)). The approach has been applied to the Libya-4 S3ETRAC acquired in the period March-June 2017. Results are given in Figure 29. These results are corrected for the known biases in the RPV030 modelling as observed when comparing against MERIS observations (Govaerts, Y., S. Sterckx, and S. Adriaensen (2013)).

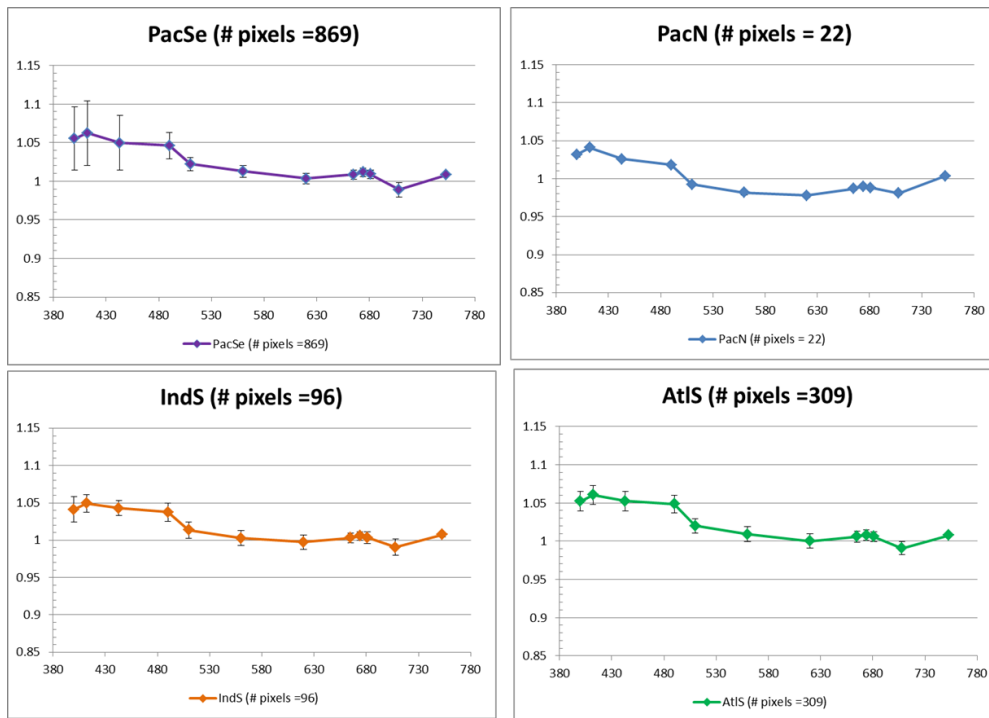


Figure 28: OSCAR Rayleigh results for April 2017

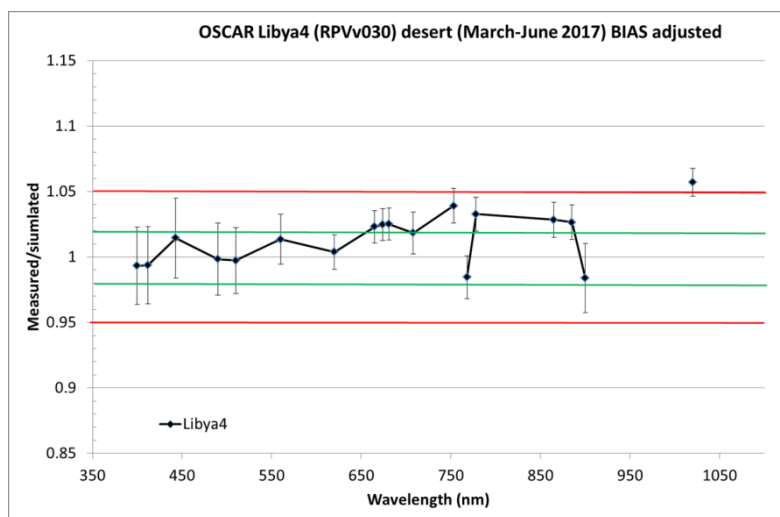



Figure 29: OSCAR Libya-4 deserts results over the period March 2017 –June 2017 in function of wavelength. Only observations with VZA less than 30° are considered. The error bars indicate the standard deviation over the 21 observations.

**References**

Govaerts, Y., S. Sterckx, and S. Adriaensen (2013). Use of simulated reflectances over bright desert target as an absolute calibration reference. Remote Sensing Letters, , Vol. 4: 6, 523-531.

	<b>Sentinel-3 MPC</b> <b>S3-A OLCI Cyclic Performance Report</b> <b>Cycle No. 019</b>	Ref.: S3MPC.ACR.PR.01-019 Issue: 1.0 Date: 19/07/2017 Page: 30
--	---	---

## 3 Level 2 Land products validation

### 3.1 [OLCI-L2LRF-CV-300]

---

There has been no update on Land products validation quantitative assessment during the cycle. Last figures (cycle 18) are considered valid.

Qualitative assessment by product inspection showed no detectable performance evolution.

### 3.2 [OLCI-L2LRF-CV-410 & OLCI-L2LRF-CV-420] – Cloud Masking & Surface Classification for Land Products

---

There has been no update on Land Cloud Masking & Surface Classification validation quantitative assessment during the cycle. Last figures (cycle 10) are considered valid.


Qualitative assessment by product inspection showed no detectable performance evolution.

### 3.3 Validation of Integrated Water Vapour over Land

---

There has been no update on Integrated Water Vapour over Land validation quantitative assessment during the cycle. Last figures (cycle 15) are considered valid.

Qualitative assessment by product inspection showed no detectable performance evolution.

	<b>Sentinel-3 MPC</b> <b>S3-A OLCI Cyclic Performance Report</b> <b>Cycle No. 019</b>	Ref.: S3MPC.ACR.PR.01-019 Issue: 1.0 Date: 19/07/2017 Page: 31
--	---	---

## 4 Level 2 Water products validation

### 4.1 [OLCI-L2-CV-210, OLCI-L2-CV-220] – Vicarious calibration of the NIR and VIS bands

---

There has been no update on SVC (System Vicarious Calibration) during Cycle 019.

### 4.2 [OLCI-L2WLR-CV-300, OLCI-L2WLR-CV-310, OLCI-L2WLR-CV-32, OLCI-L2WLR-CV-330, OLCI-L2WLR-CV-340, OLCI-L2WLR-CV-350, OLCI-L2WLR-CV-360 and OLCI-L2WLR-CV-370] – Level 2 Water-leaving Reflectance product validation.

---

#### Activities done

- ❖ The focus for this time period has been on the Near Real Time data.
- ❖ All extractions and statistics have been regenerated for the last three months (April 1<sup>st</sup> 2017 onward; rolling archive limitation). The available matchups therefore cover the spring situation as most of the stations are in the northern hemisphere. Time range available for last processing period covered February 1<sup>st</sup> to April 30<sup>th</sup>.
- ❖ MOBY and AERONET-OC in-situ data are available for this time period.

**WARNING:** the results presented below contain several processing baselines. Notably, the most recent baseline contains System Vicarious Calibration gains, with a significant impact on the water-leaving reflectances. However this processing baseline went operational early July (July 4<sup>th</sup> onward), the impact is therefore fairly small on the statistics.

#### Overall Water-leaving Reflectance performance

Figure 30 below presents the scatter plots with statistics of OLCI versus in situ reflectances computed for the NRT dataset covering the period from May 1<sup>st</sup> 2016 to July 9<sup>th</sup> 2017. As stated in previous reports a positive bias is visible particularly on 412 and 443. Table 2 to Table 5 below summarises the statistics over the latest reporting periods, confirming the important bias at 412 and 443nm. The statistics of the current NRT period are presented in Table 5. Figures remain similar between the two periods. However the different statistical parameters tend to improve from December to present. Most AERONET-OC being in the northern hemisphere, this might be a consequent of less complex coastal water optical properties (calm seas, less turbid river discharge) and more simple atmosphere (See time series

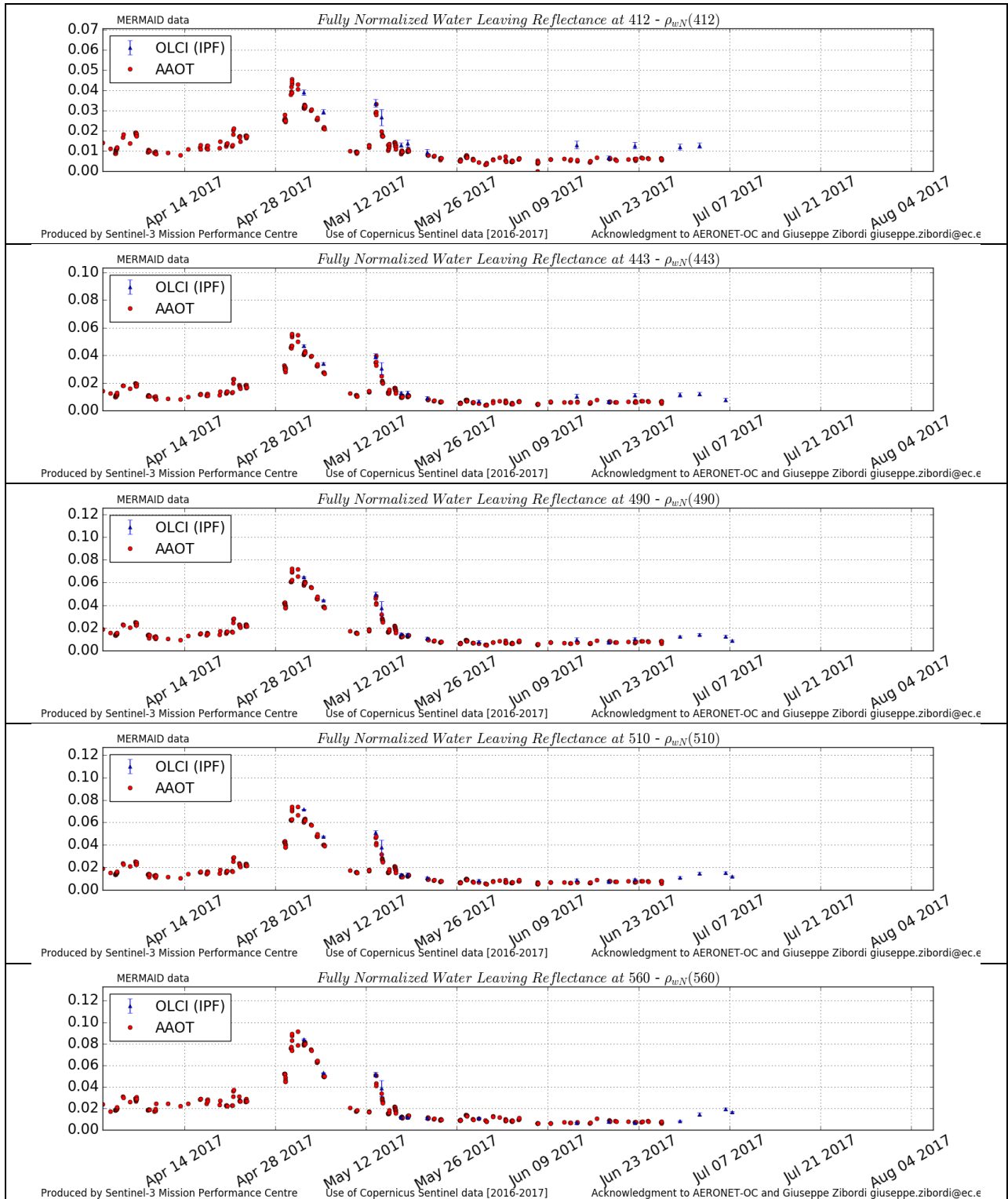


Figure 31 with stable radiometric properties since mid may on AAOT)



## Sentinel-3 MPC

### S3-A OLCI Cyclic Performance Report

Cycle No. 019

Ref.: S3MPC.ACR.PR.01-019

Issue: 1.0

Date: 19/07/2017

Page: 33

**Table 2: statistics over December 2016-March 2017 reporting period**

lambda	N	RPD	RPD	MAD	RMSE	slope	int.	r2
412	25	70,55%	77,47%	0,0055	0,0071	0,9486	0,0061	0,6787
443	25	43,34%	44,27%	0,0045	0,0056	1,1251	0,0028	0,9037
490	24	28,53%	28,53%	0,0048	0,0059	1,1634	0,0016	0,9611
510	2	31,69%	31,69%	0,0091	0,0093	2,0459	-0,0207	1,0000
560	17	15,44%	16,95%	0,0037	0,0052	1,1350	0,0003	0,9655
665	25	10,56%	34,24%	0,0010	0,0032	1,3661	-0,0013	0,9236

**Table 3: statistics over February 2017-April 2017 reporting period**

lambda	N	RPD	RPD	MAD	RMSE	slope	int.	r2
412	60	88.15%	93.77%	0.0052	0.0066	1.0404	0.0048	0.6176
443	60	46.70%	50.43%	0.0038	0.0049	1.1195	0.0026	0.8046
490	59	31.38%	32.56%	0.0039	0.0046	1.1397	0.0019	0.9263
510	19	27.06%	27.06%	0.0050	0.0055	1.1474	0.0021	0.9486
560	53	13.42%	16.58%	0.0024	0.0035	1.1281	0.0001	0.9379
665	51	1.02%	29.79%	0.0000	0.0012	1.0202	-0.0001	0.7892

**Table 4 statistics over April 2017-June 2017 reporting period**

lambda	N	RPD	RPD	MAD	RMSE	slope	intercept	r2
400	2	17.9%	17.9%	0.0088	0.0100	-2.3992	0.1784	1.0000
412	15	66.3%	66.3%	0.0055	0.0062	1.0618	0.0046	0.9611
443	15	36.7%	37.0%	0.0037	0.0044	1.1107	0.0023	0.9454
490	20	32.1%	32.3%	0.0038	0.0044	1.0153	0.0036	0.8224
510	10	35.9%	35.9%	0.0045	0.0048	0.8626	0.0064	0.7505
560	21	17.0%	21.9%	0.0020	0.0034	1.0925	0.0006	0.9205

**Table 5: statistics over the current reporting period (May 1<sup>st</sup> to July 10<sup>th</sup>)**

lambda	N	RPD	RPD	MAD	RMSE	slope	intercept	r2
412	35	30.5%	38.2%	0.0025	0.0060	0.9699	0.0033	0.9364
443	43	25.2%	32.9%	0.0023	0.0061	1.0444	0.0012	0.9546
490	52	15.2%	22.2%	0.0020	0.0055	1.0462	0.0007	0.9756
510	21	24.1%	24.9%	0.0026	0.0039	1.1577	0.0004	0.9946
560	52	2.4%	11.1%	0.0004	0.0045	1.0196	-0.0002	0.9701
665	32	-6.9%	17.7%	-0.0002	0.0023	0.9830	-0.0001	0.8423



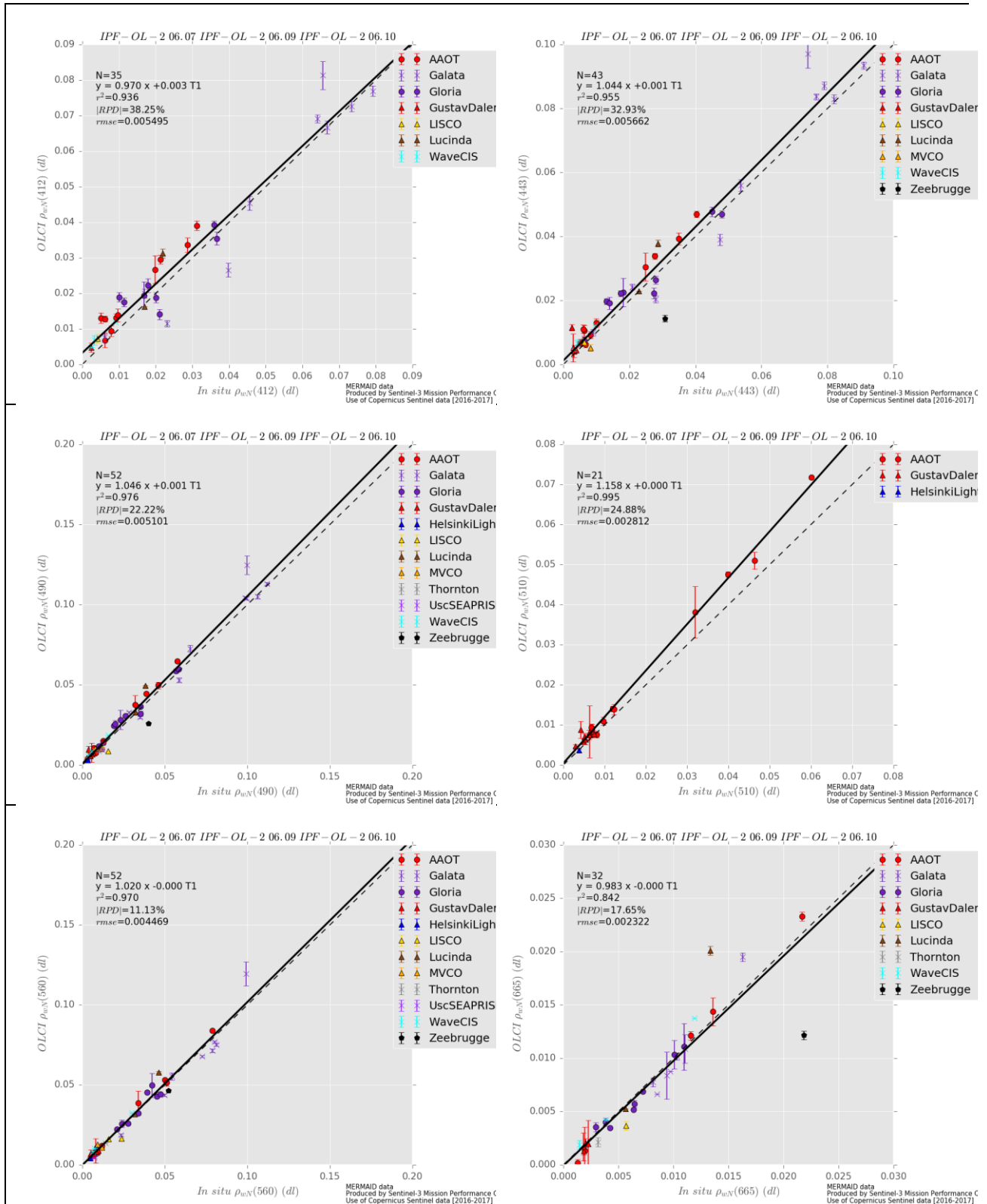


Figure 30: Scatter plots of OLCI versus in situ radiometry

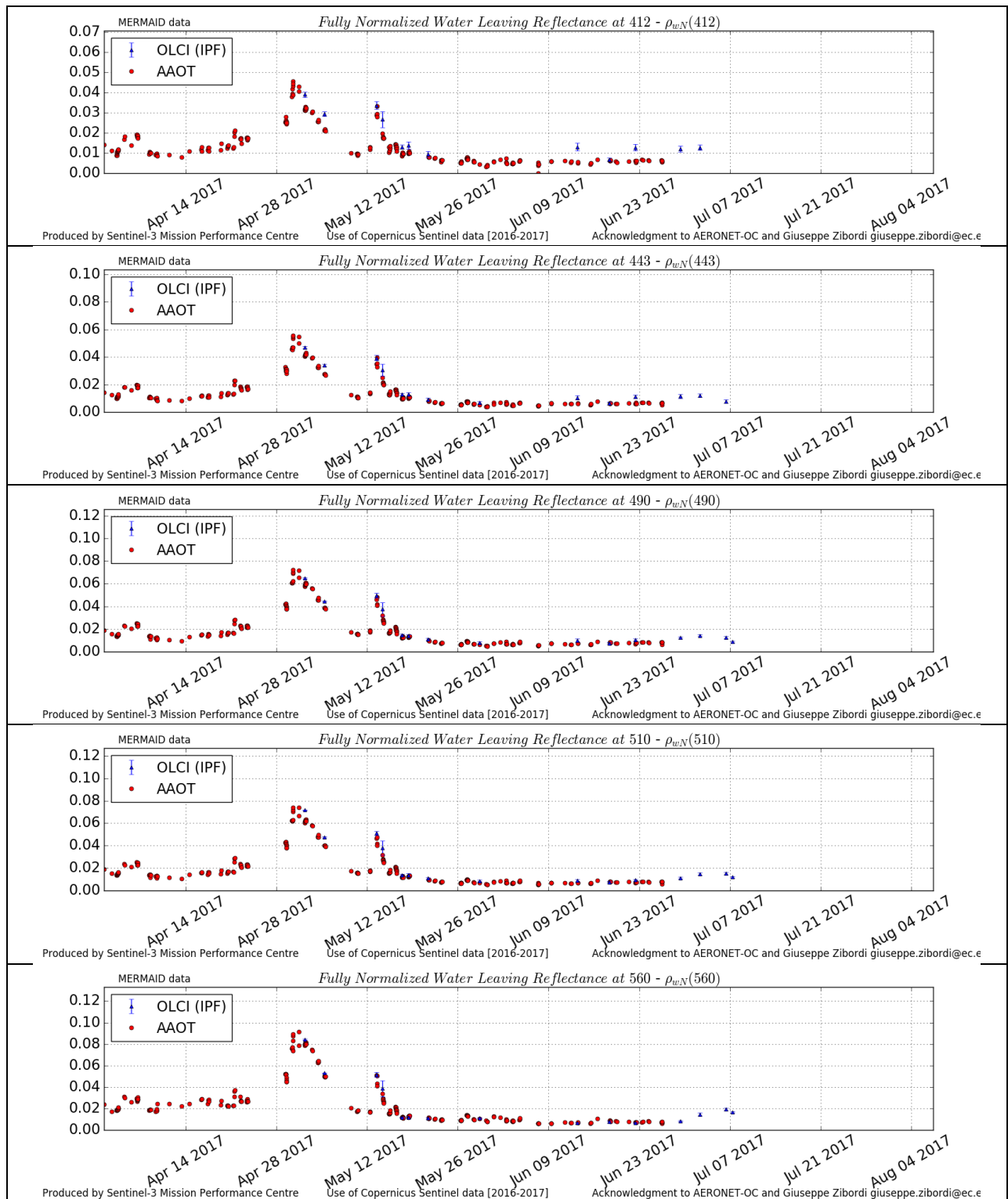


Figure 31 and Figure 32 below show the AAOT and Galata time series derived over the current NRT period. The general cycle on in situ data is well reproduced but these time series confirm the positive bias at 412 and 443nm. The Galata station display a significant elevation of the radiometric signal from May to early July, from Figure 33, it is difficult to certify if it is a chlorophyll bloom or a sediment discharge.



# Sentinel-3 MPC

## S3-A OLCI Cyclic Performance Report

### Cycle No. 019

Ref.: S3MPC.ACR.PR.01-019  
Issue: 1.0  
Date: 19/07/2017  
Page: 36

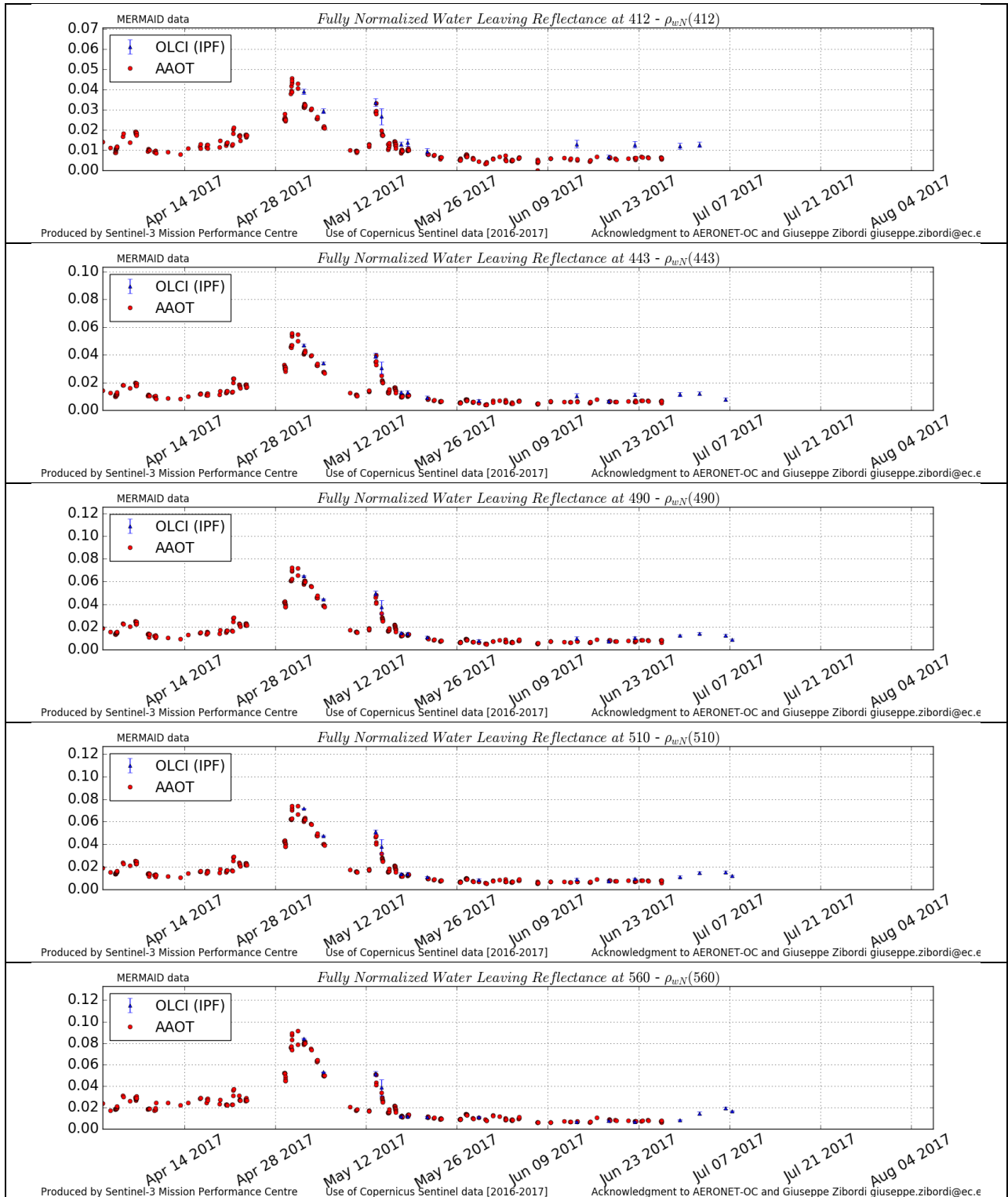


Figure 31: OLCI and AERONET-OC radiometric time series AAOT station.



# Sentinel-3 MPC

## S3-A OLCI Cyclic Performance Report

### Cycle No. 019

Ref.: S3MPC.ACR.PR.01-019  
Issue: 1.0  
Date: 19/07/2017  
Page: 37

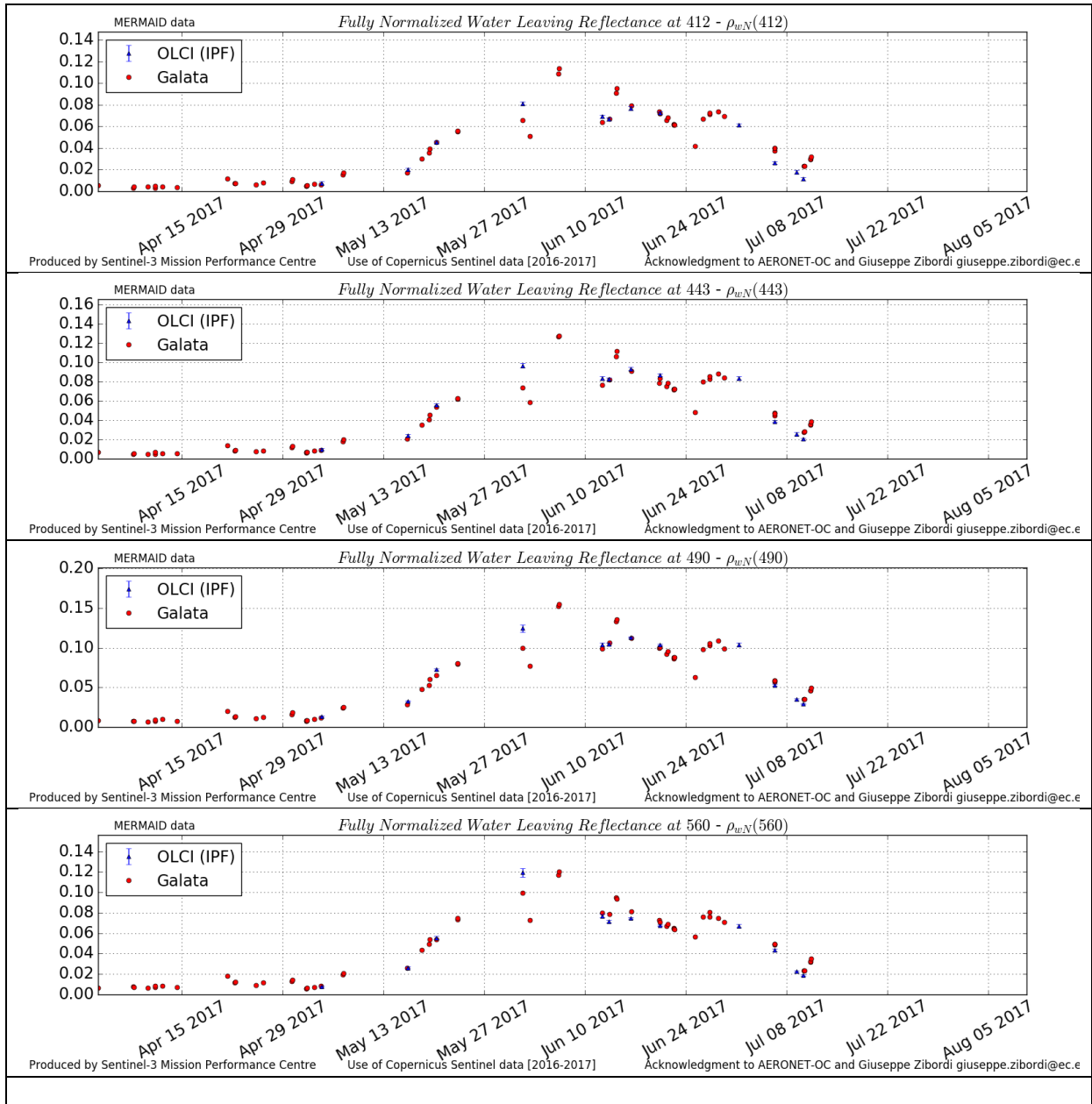
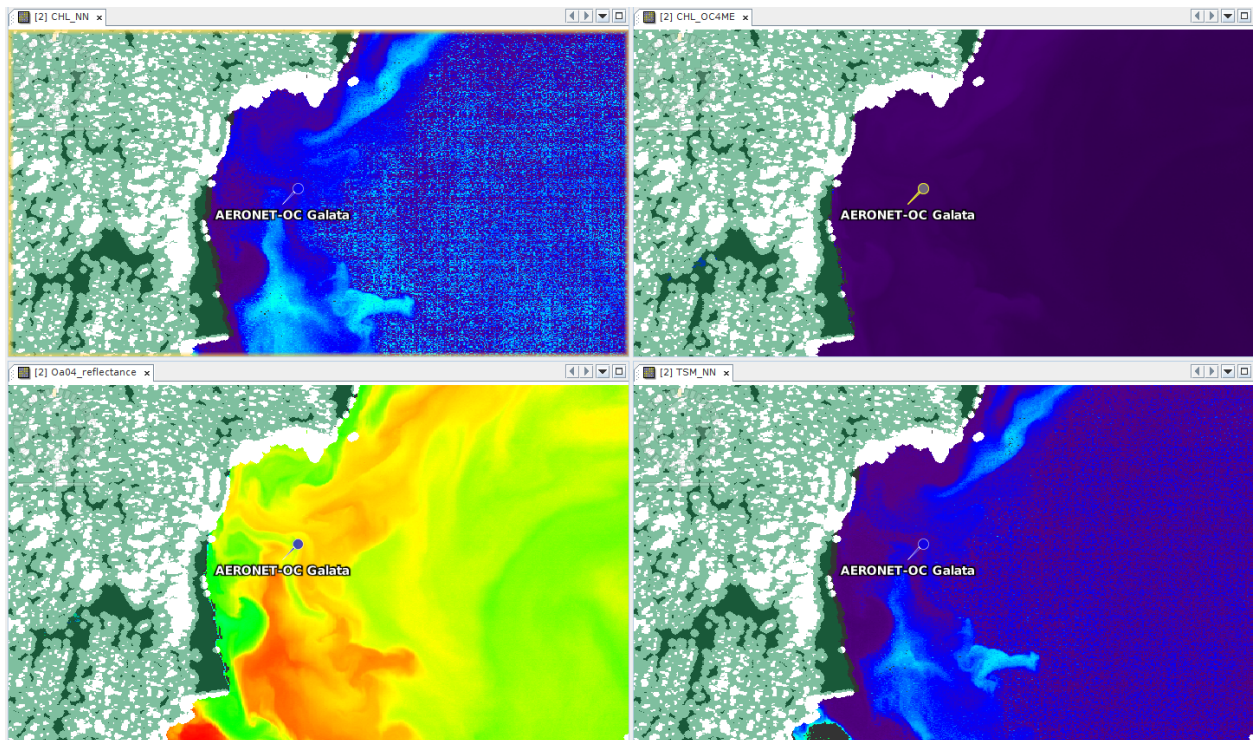


Figure 32: OLCI and AERONET-OC radiometric time series Galata station.




*Figure 33: OLCI overpath of Galata station (20170612). Chl-NN top left, CHL\_OC4Me, top right, reflectance at 490nm bottom left, TSM-NN bottom right*

### 4.3 [OLCI-L2WLR-CV530] Validation of Aerosol Product

There has been no update on Aerosol Products validation quantitative assessment during the cycle. Last figures (cycle 18) are considered valid.

Qualitative assessment by product inspection showed no detectable performance evolution.

	<b>Sentinel-3 MPC</b> <b>S3-A OLCI Cyclic Performance Report</b> <b>Cycle No. 019</b>	Ref.: S3MPC.ACR.PR.01-019 Issue: 1.0 Date: 19/07/2017 Page: 39
--	---	---


## 5 Level 2 SYN products validation

### 5.1 [SYN-L2-CV-100]

---

There has been no update on SYN products validation quantitative assessment during the cycle. Last figures (cycle 10) are considered valid.


Qualitative assessment by product inspection showed no detectable performance evolution.

	<b>Sentinel-3 MPC</b> <b>S3-A OLCI Cyclic Performance Report</b> <b>Cycle No. 019</b>	Ref.: S3MPC.ACR.PR.01-019 Issue: 1.0 Date: 19/07/2017 Page: 40
--	---	---

## 6 Events

One OLCI Radiometric Calibration Sequence has been acquired during Cycle 019:

- ❖ S01 sequence on 28/05/2017 20:35 to 20:37 (absolute orbit 6653)

	<b>Sentinel-3 MPC</b> <b>S3-A OLCI Cyclic Performance Report</b> <b>Cycle No. 019</b>	Ref.: S3MPC.ACR.PR.01-019 Issue: 1.0 Date: 19/07/2017 Page: 41
--	---	---

## 7 Appendix A

Other reports related to the Optical mission are:

- ❖ S3-A SLSTR Cyclic Performance Report, Cycle No. 019 (ref. S3MPC.RAL.PR.02-019)

All Cyclic Performance Reports are available on MPC pages in Sentinel Online website, at:  
<https://sentinel.esa.int>

***End of document***